The background of the slide features a repeating pattern of large, light-green spheres and smaller, light-orange cylinders. The cylinders are oriented vertically, with some appearing to pass through the spheres. The overall composition is abstract and geometric.

Measuring the Gluon Spin Distribution at Small-x (Part 2: Detector)

Mickey Chiu
BROOKHAVEN
NATIONAL LABORATORY

Muon Spectrometer

Muon

Neutrino

Hadronic Calorimeter

Proton

Neutron

The dashed tracks are invisible to the detector

Electromagnetic Calorimeter

Electron

Photon

Solenoid magnet

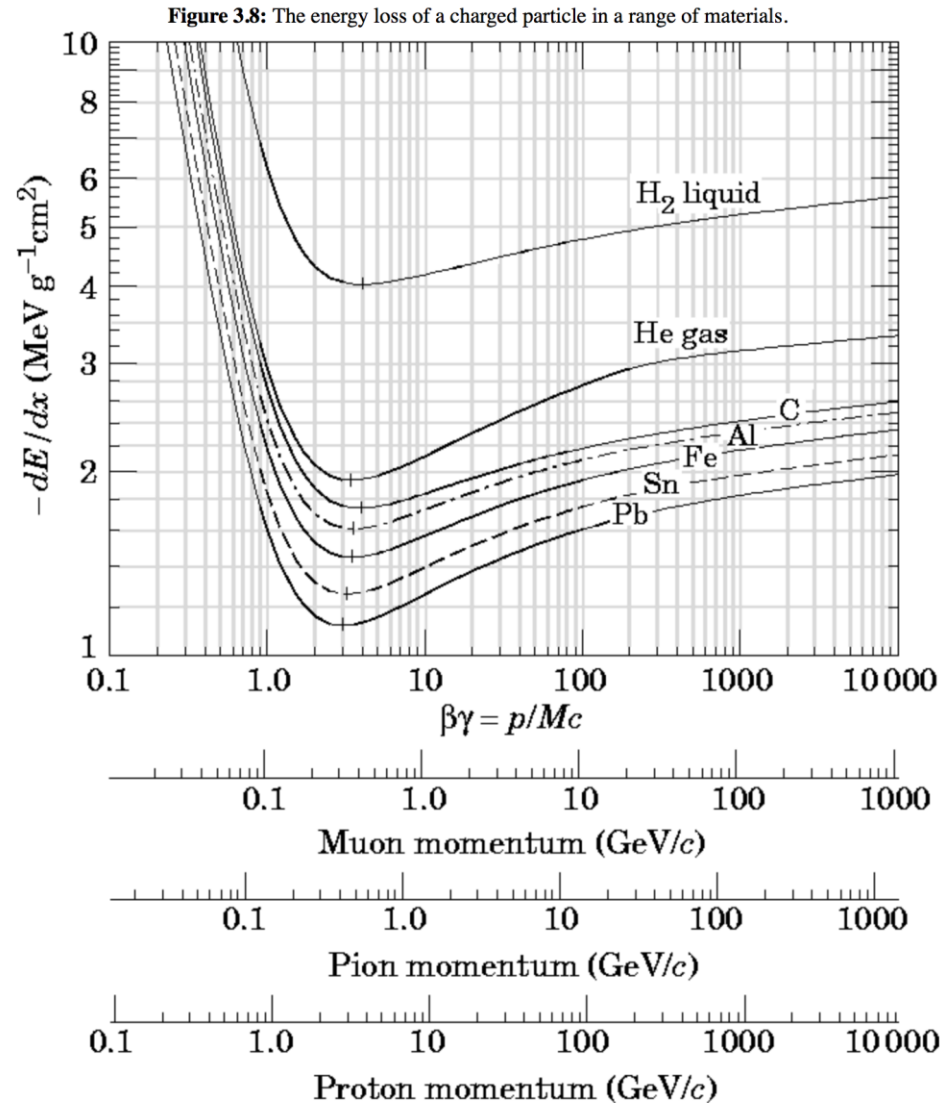
Tracking {
Transition
Radiation
Tracker

Pixel/SCT
detector



<http://atlas.ch>

Ionization Loss of Charged Particles in Matter



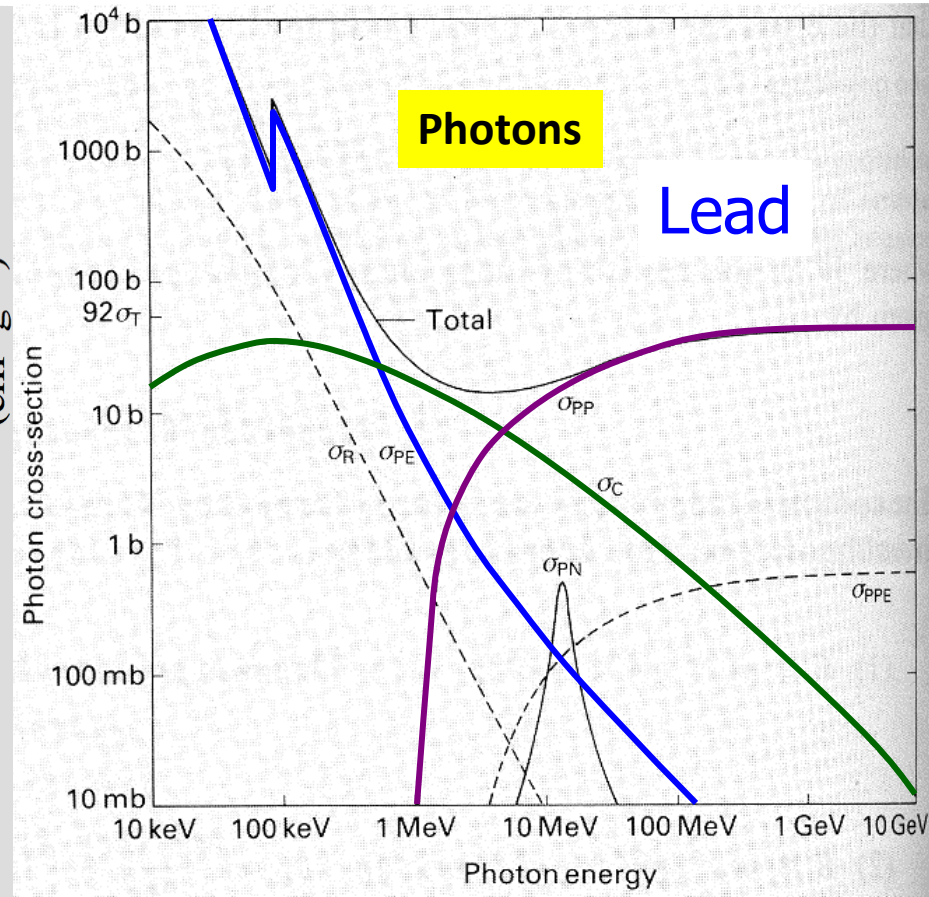
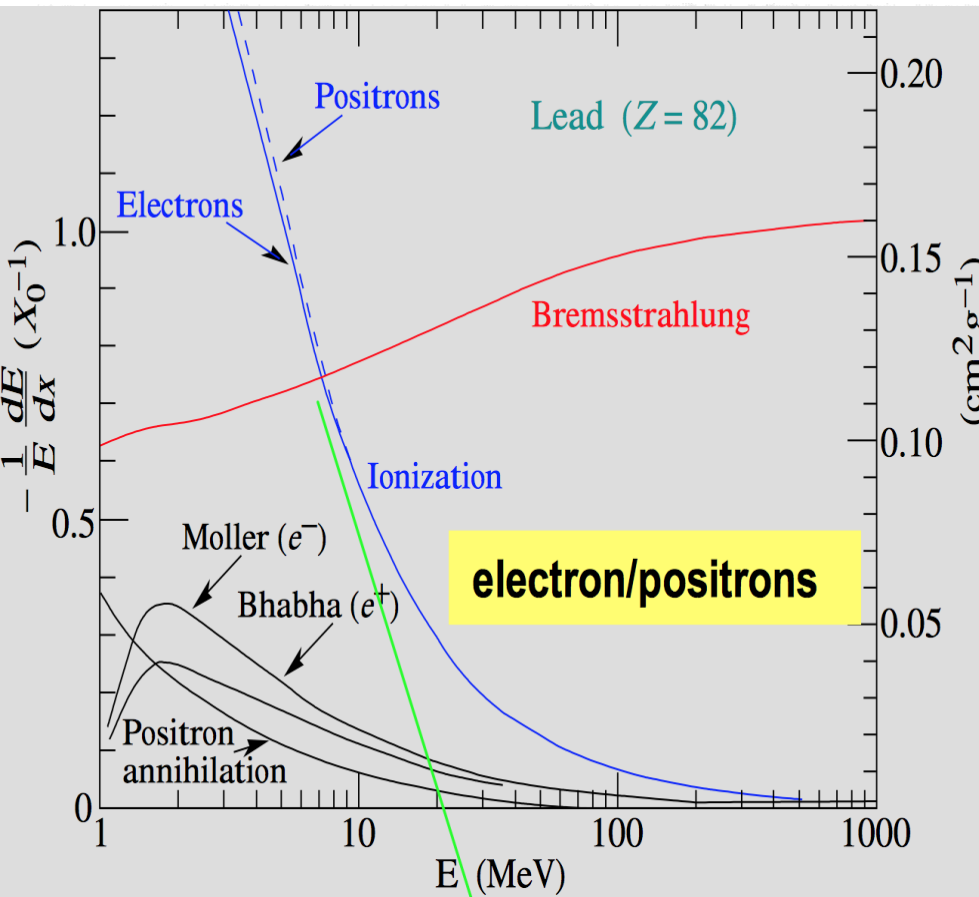
- Bethe-Bloch Equation... Coulomb interaction with the electrons in the atoms

13.1 Photons in matter

(Overview)

- Rayleigh scattering
 - Coherent, elastic scattering of the entire atom (the blue sky)
 - $\gamma + \text{atom} \rightarrow \gamma + \text{atom}$
 - dominant at $\lambda_\gamma > \text{size of atoms}$
- Compton scattering
 - Incoherent scattering of electron from atom
 - $\gamma + e^-_{\text{bound}} \rightarrow \gamma + e^-_{\text{free}}$
 - possible at all $E_\gamma > \min(E_{\text{bind}})$
 - to properly call it Compton requires $E_\gamma > E_{\text{bind}}(e^-)$ to approximate free e^-
- Photoelectric effect
 - absorption of photon and ejection of single atomic electron
 - $\gamma + \text{atom} \rightarrow \gamma + e^-_{\text{free}} + \text{ion}$
 - possible for $E_\gamma < \max(E_{\text{bind}}) + \delta E(E_{\text{atomic-recoil}}, \text{line width})$ (just above k-edge)
- Pair production
 - absorption of γ in atom and emission of e^+e^- pair
 - Two varieties:
 - $\gamma + \text{nucleus} \rightarrow e^+ + e^- + \text{nucleus}$ (more momentum transfer to nucleus \rightarrow dominates)
 - $\gamma + Z \text{ atomic electrons} \rightarrow e^+ + e^- + Z \text{ atomic electrons}$
 - both summarised via: $g + g(\text{virtual}) \rightarrow e^+ + e^-$
 - Needs $E_\gamma > 2m_e c^2$
 - Nucleus has to recoil to conserve momentum \rightarrow coupling to nucleus needed \rightarrow strongly Z-dependent cross section

Electromagnetic Interactions in Matter



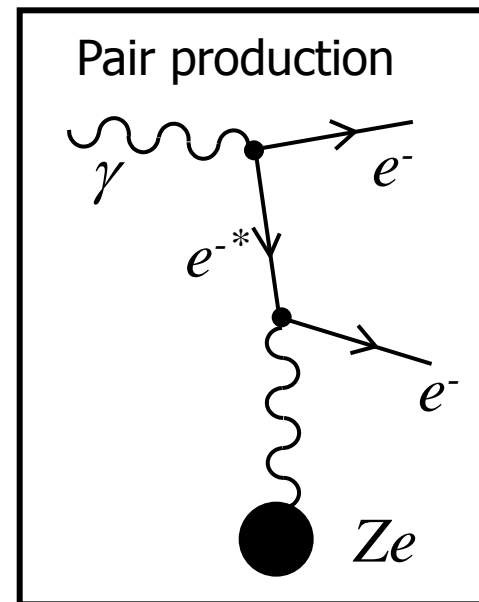
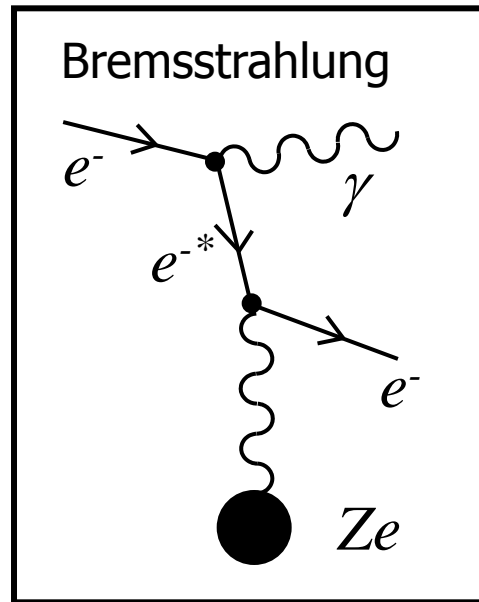
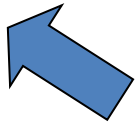
- R → Rayleigh
- PE → Photoeffect
- C → Compton
- PP → Pair Production
- PPE → Pair Production on atomic electrons
- PN → Giant Photo-Nuclear dipole resonance

13.1 Photons in matter

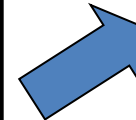
(Note on Pair Production)

- Compare pair production with Bremsstrahlung

Typical Lenth =
Radiation Length
 X_0



Typical Lenth =
Pair Production
Length L_0



- Very similar Feynman Diagram
- Just two arms swapped

$$L_0 = \frac{9}{7} X_0$$

Electromagnetic showers

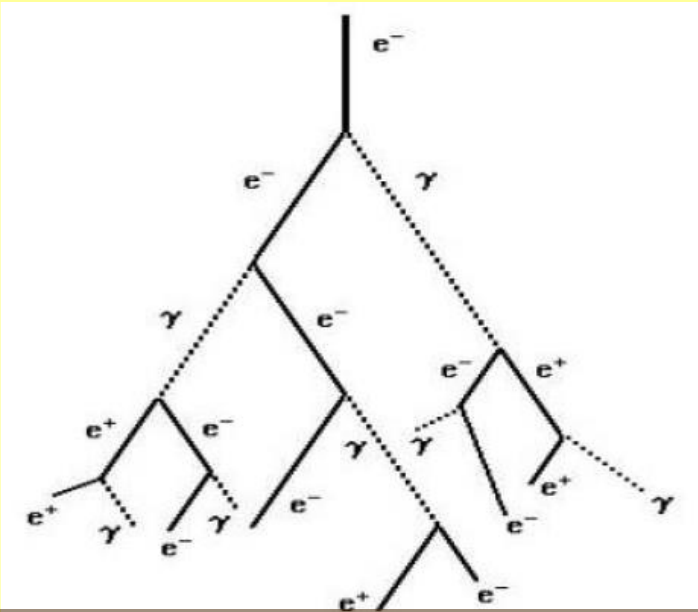
(A) Bremsstrahlung

radiation of real photons in the Coulomb field of nuclei

$$-\frac{dE}{dx} = 4\alpha \cdot N_A \cdot \frac{Z^2}{A} \cdot z^2 \cdot \left(\frac{1}{4\pi\epsilon_0} \frac{e^2}{mc^2} \right) \cdot \ln\left(\frac{183}{Z^{1/3}}\right) \cdot E$$

(B) Pair production

needs additional mass for momentum conservation

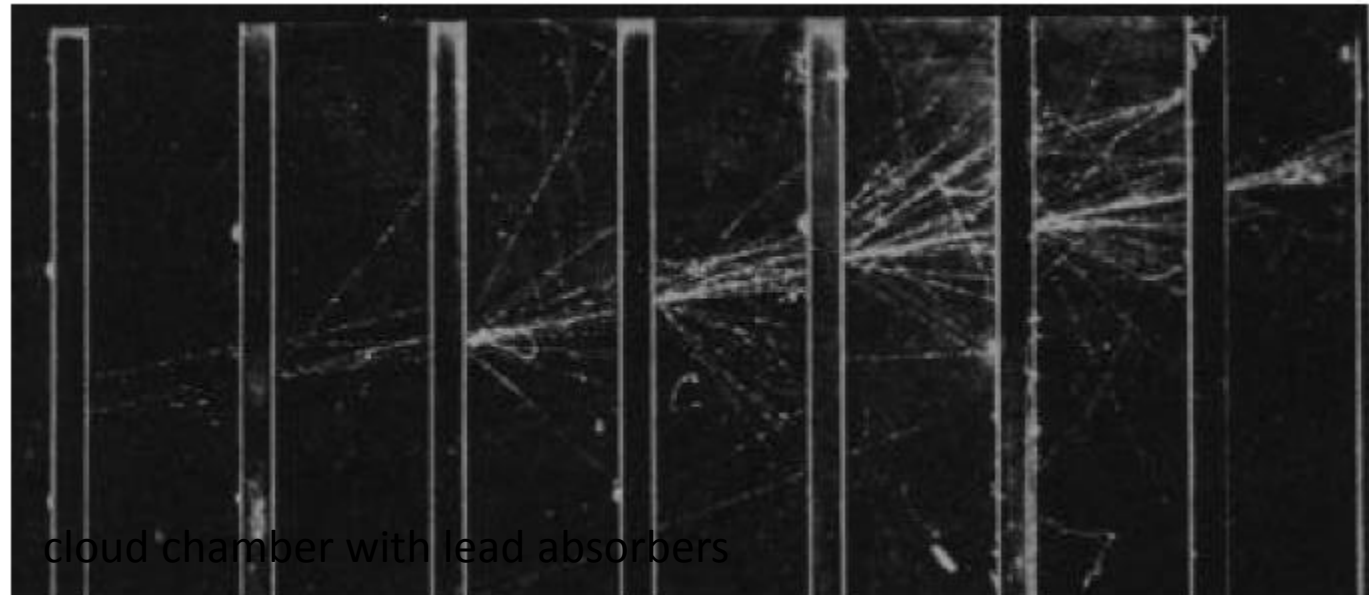


$$X_0 = \frac{A}{4\alpha \cdot N_A Z^2 r_e^2 \ln\left(\frac{183}{Z^{1/3}}\right)}$$

$$\lambda_{pair} = \frac{7}{9} X_0$$

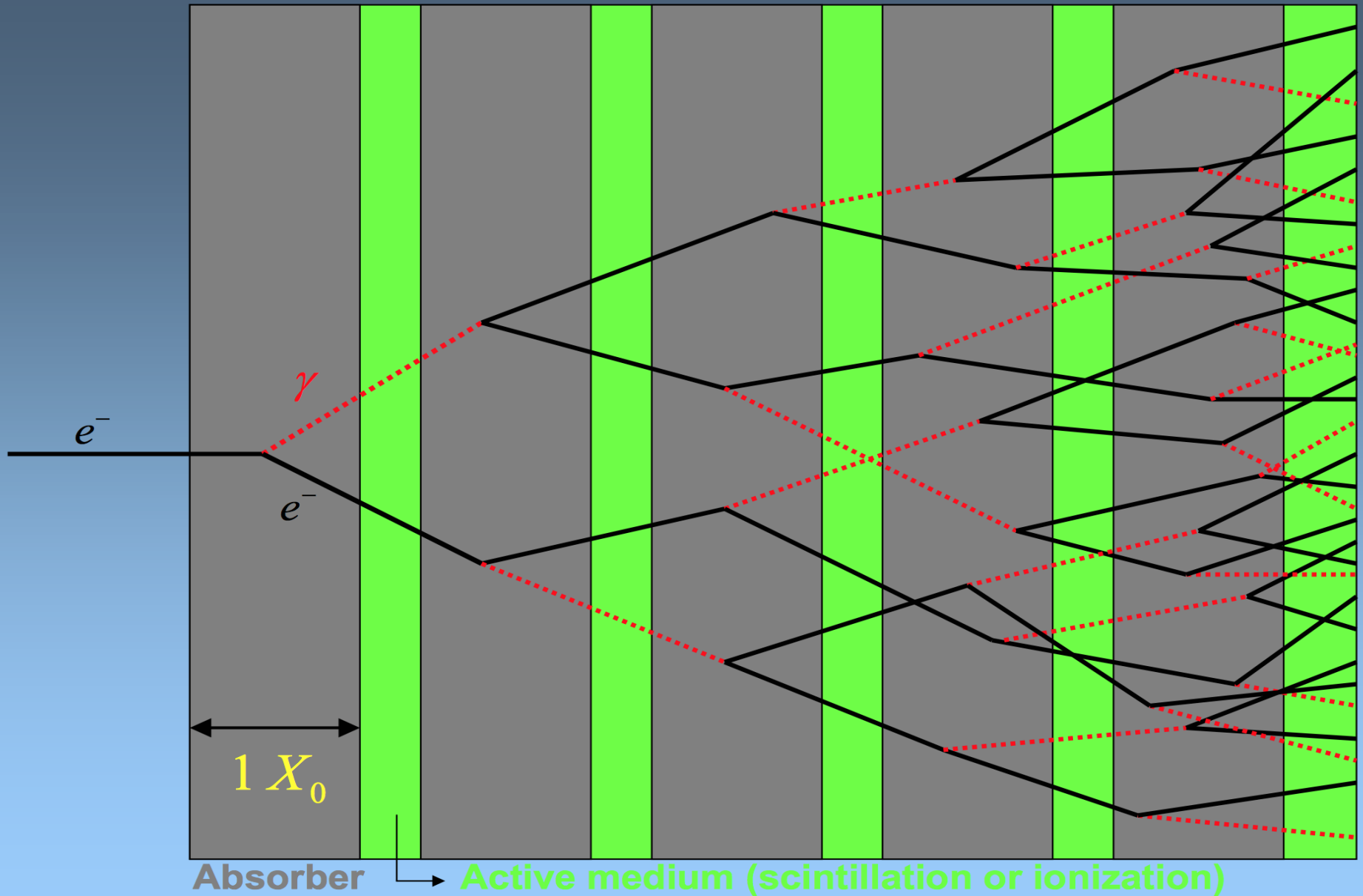
Moliere radius

$$R_M = X_0 \frac{21 \text{ MeV}}{E_C}$$



cloud chamber with lead absorbers

Electromagnetic Shower



Electromagnetic showers

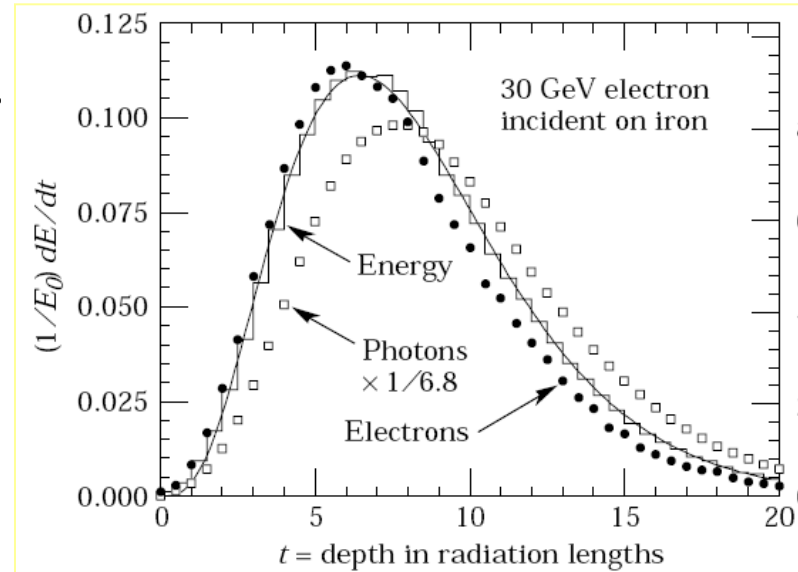
The shower development is a statistical process.

α - Active sampling wrt total detector volume

β - Uniformity of the detector, non-linearities

Energy resolution

$$\frac{\sigma_E}{E} \approx \frac{\alpha}{\sqrt{E}} \oplus \beta$$

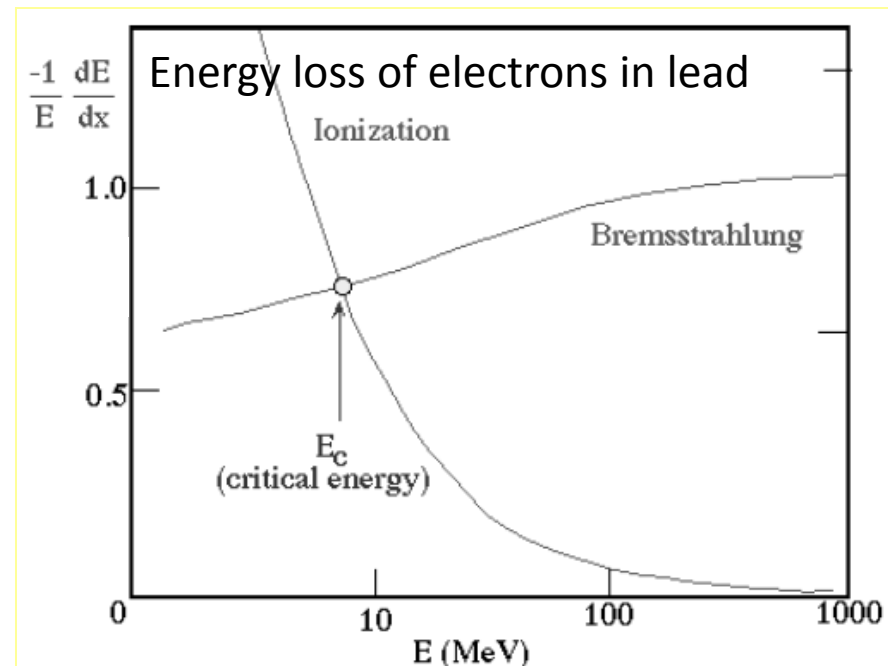


Critical energy

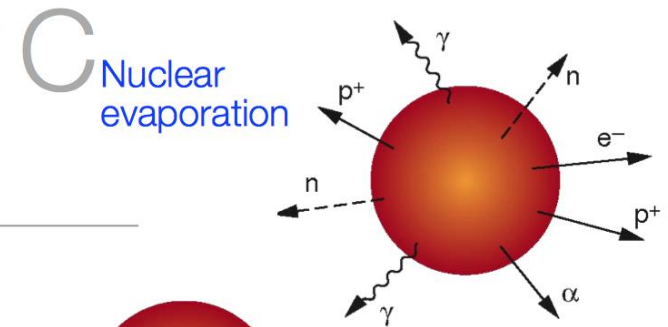
$$\left. \frac{dE}{dx}(E_C) \right|_{\text{Brems}} = \left. \frac{dE}{dx}(E_C) \right|_{\text{ion}}$$

Shower maximum depth

$$t_{\max} = \frac{\ln(E_0/E_C)}{\ln 2}$$

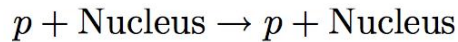


Hadronic Showers

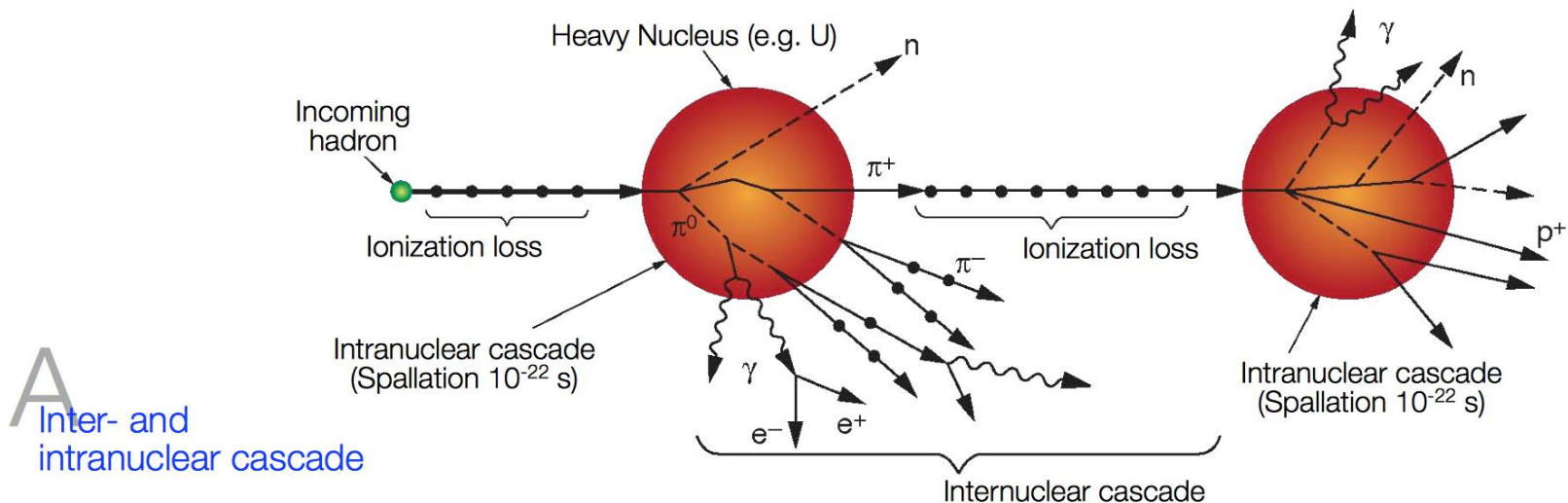
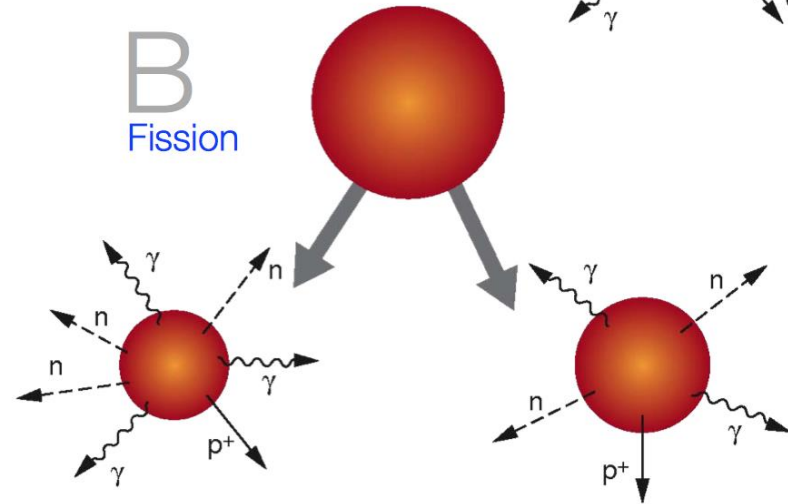
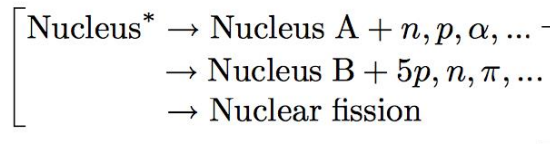
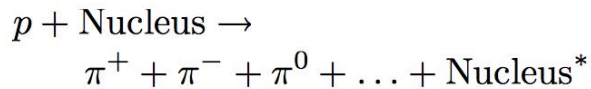


Hadronic interaction:

Elastic:



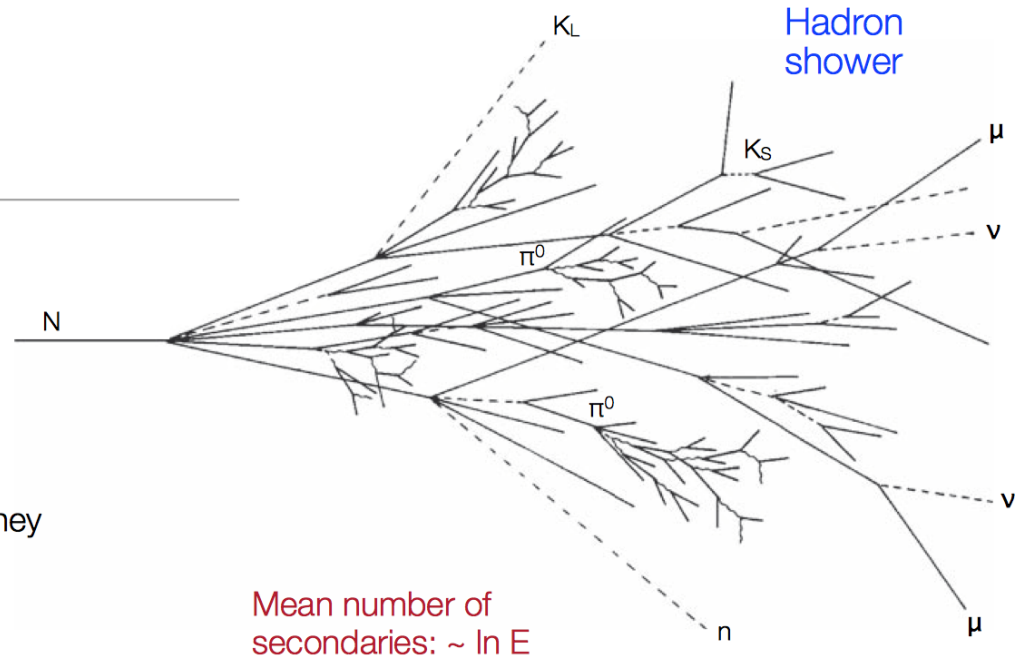
Inelastic:



Hadronic Showers

Shower development:

1. $p + \text{Nucleus} \rightarrow \text{Pions} + N^* + \dots$
2. Secondary particles ...
undergo further inelastic collisions until they
fall below pion production threshold
3. Sequential decays ...
 $\pi_0 \rightarrow \gamma\gamma$: yields electromagnetic shower
 Fission fragments $\rightarrow \beta$ -decay, γ -decay
 Neutron capture \rightarrow fission
 Spallation ...



Substantial
electromagnetic fraction

$$f_{\text{em}} \sim \ln E$$

[variations significant]

Cascade energy distribution:

[Example: 5 GeV proton in lead-scintillator calorimeter]

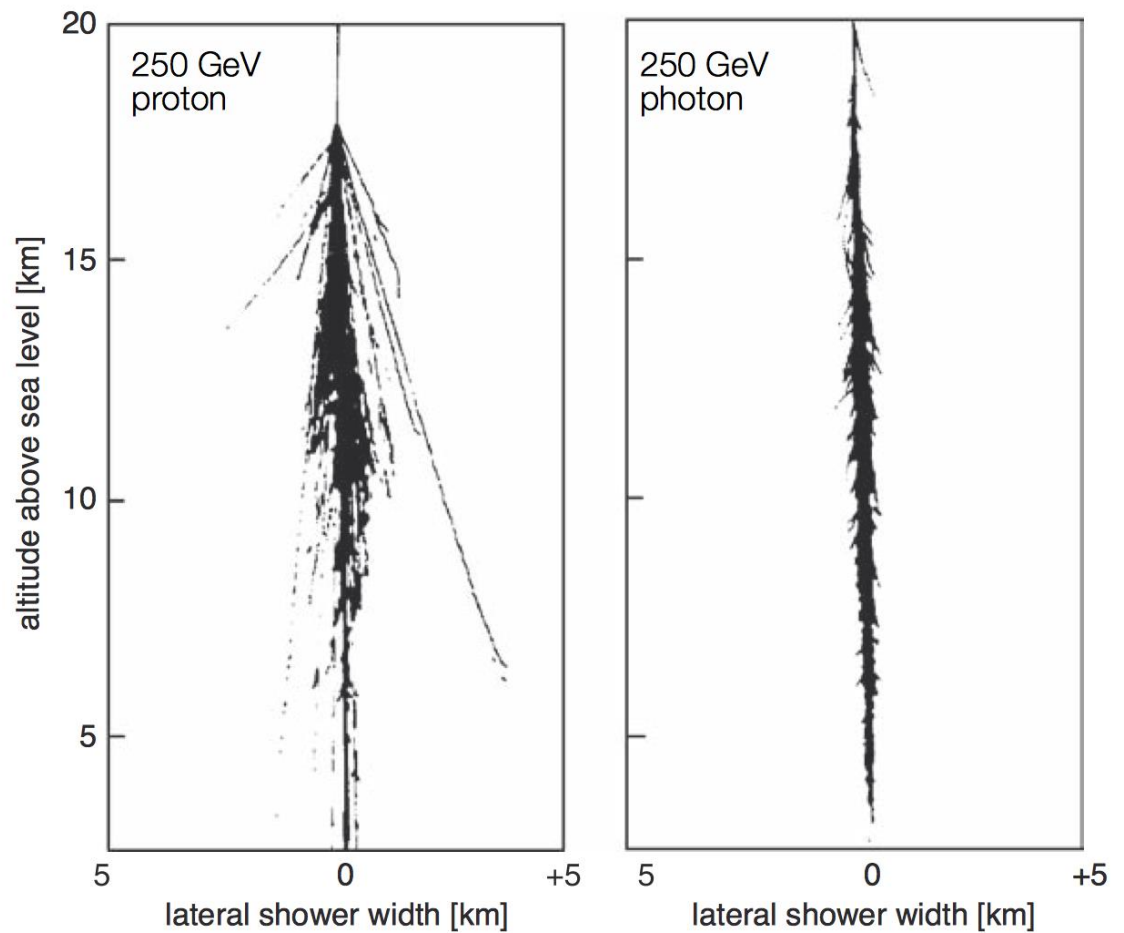
Ionization energy of charged particles (p, π , μ)	1980 MeV [40%]
Electromagnetic shower (π^0 , η^0 , e)	760 MeV [15%]
Neutrons	520 MeV [10%]
Photons from nuclear de-excitation	310 MeV [6%]
Non-detectable energy (nuclear binding, neutrinos)	1430 MeV [29%]
	<hr/>
	5000 MeV [29%]

Hadronic Showers

Comparison

hadronic vs electromagnetic shower ...

[Simulated air showers]



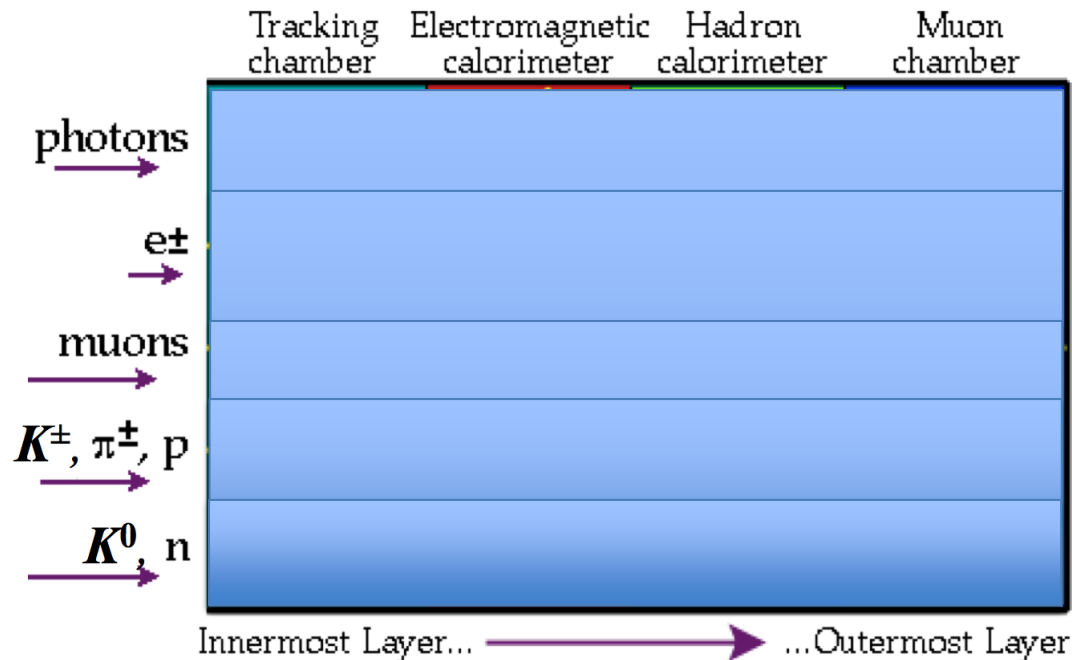
6. ATOMIC AND NUCLEAR PROPERTIES OF MATERIALS

Table 6.1 Abridged from pdg.lbl.gov/AtomicNuclearProperties by D. E. Groom (2007). See web pages for more detail about entries in this table including chemical formulae, and for several hundred other entries. Quantities in parentheses are for NTP (20° C and 1 atm), and square brackets indicate quantities evaluated at STP. Boiling points are at 1 atm. Refractive indices n are evaluated at the sodium D line blend (589.2 nm); values $\gg 1$ in brackets are for $(n - 1) \times 10^6$ (gases).

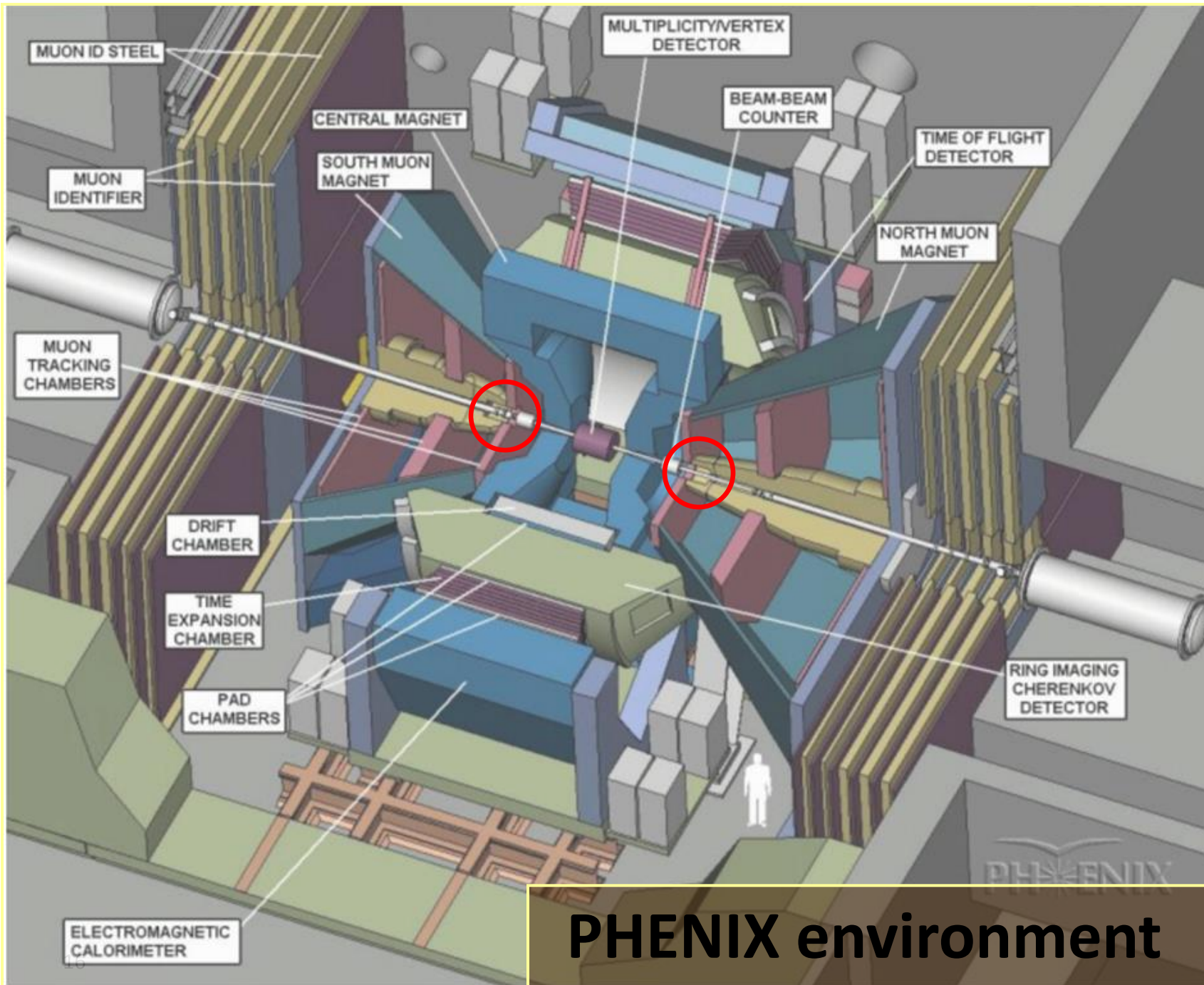
Material	Z	A	$\langle Z/A \rangle$	Nucl.coll. length λ_T {g cm ⁻² }	Nucl.inter. length λ_I {g cm ⁻² }	Rad.len. X_0 {g cm ⁻² }	$dE/dx _{\min}$ { MeV g ⁻¹ cm ² }	Density {g cm ⁻³ } ({gℓ ⁻¹ })	Melting point (K)	Boiling point (K)	Refract. index (@ Na D)
H ₂	1	1.00794(7)	0.99212	42.8	52.0	63.04	(4.103)	0.071(0.084)	13.81	20.28	1.11[132.]
D ₂	1	2.01410177803(8)	0.49650	51.3	71.8	125.97	(2.053)	0.169(0.168)	18.7	23.65	1.11[138.]
He	2	4.002602(2)	0.49967	51.8	71.0	94.32	(1.937)	0.125(0.166)		4.220	1.02[35.0]
Li	3	6.941(2)	0.43221	52.2	71.3	82.78	1.639	0.534	453.6	1615.	
Be	4	9.012182(3)	0.44384	55.3	77.8	65.19	1.595	1.848	1560.	2744.	
C diamond	6	12.0107(8)	0.49955	59.2	85.8	42.70	1.725	3.520			2.42
C graphite	6	12.0107(8)	0.49955	59.2	85.8	42.70	1.742	2.210			
N ₂	7	14.0067(2)	0.49976	61.1	89.7	37.99	(1.825)	0.807(1.165)	63.15	77.29	1.20[298.]
O ₂	8	15.9994(3)	0.50002	61.3	90.2	34.24	(1.801)	1.141(1.332)	54.36	90.20	1.22[271.]
F ₂	9	18.9984032(5)	0.47372	65.0	97.4	32.93	(1.676)	1.507(1.580)	53.53	85.03	[195.]
Ne	10	20.1797(6)	0.49555	65.7	99.0	28.93	(1.724)	1.204(0.839)	24.56	27.07	1.09[67.1]
Al	13	26.9815386(8)	0.48181	69.7	107.2	24.01	1.615	2.699	933.5	2792.	
Si	14	28.0855(3)	0.49848	70.2	108.4	21.82	1.664	2.329	1687.	3538.	3.95
Cl ₂	17	35.453(2)	0.47951	73.8	115.7	19.28	(1.630)	1.574(2.980)	171.6	239.1	[773.]
Ar	18	39.948(1)	0.45059	75.7	119.7	19.55	(1.519)	1.396(1.662)	83.81	87.26	1.23[281.]
Ti	22	47.867(1)	0.45961	78.8	126.2	16.16	1.477	4.540	1941.	3560.	
Fe	26	55.845(2)	0.46557	81.7	132.1	13.84	1.451	7.874	1811.	3134.	
Cu	29	63.546(3)	0.45636	84.2	137.3	12.86	1.403	8.960	1358.	2835.	
Ge	32	72.64(1)	0.44053	86.9	143.0	12.25	1.370	5.323	1211.	3106.	
Sn	50	118.710(7)	0.42119	98.2	166.7	8.82	1.263	7.310	505.1	2875.	
Xe	54	131.293(6)	0.41129	100.8	172.1	8.48	(1.255)	2.953(5.483)	161.4	165.1	1.39[701.]
W	74	183.84(1)	0.40252	110.4	191.9	6.76	1.145	19.300	3695.	5828.	
Pt	78	195.084(9)	0.39983	112.2	195.7	6.54	1.128	21.450	2042.	4098.	
Au	79	196.966569(4)	0.40108	112.5	196.3	6.46	1.134	19.320	1337.	3129.	
Pb	82	207.2(1)	0.39575	114.1	199.6	6.37	1.122	11.350	600.6	2022.	
U	92	[238.02891(3)]	0.38651	118.6	209.0	6.00	1.081	18.950	1408.	4404.	
Air (dry, 1 atm)			0.49919	61.3	90.1	36.62	(1.815)	(1.205)		78.80	
Shielding concrete			0.50274	65.1	97.5	26.57	1.711	2.300			
Borosilicate glass (Pyrex)			0.49707	64.6	96.5	28.17	1.696	2.230			
Lead glass			0.42101	95.9	158.0	7.87	1.255	6.220			
Standard rock			0.50000	66.8	101.3	26.54	1.688	2.650			

Interactions with Matter

- Generally a detector consists of a tracking detector , an electromagnetic and hadron calorimeter and muon chambers in a magnetic field.
- Each experiment uses different technologies to construct the sub-detectors.

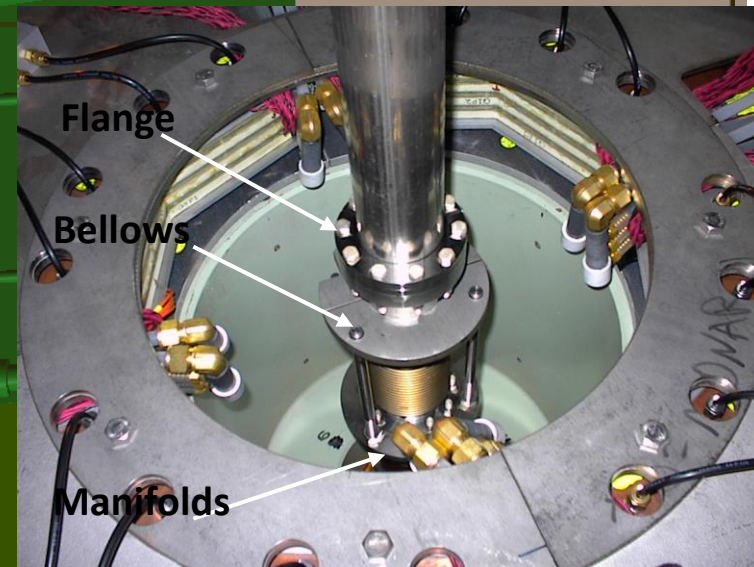
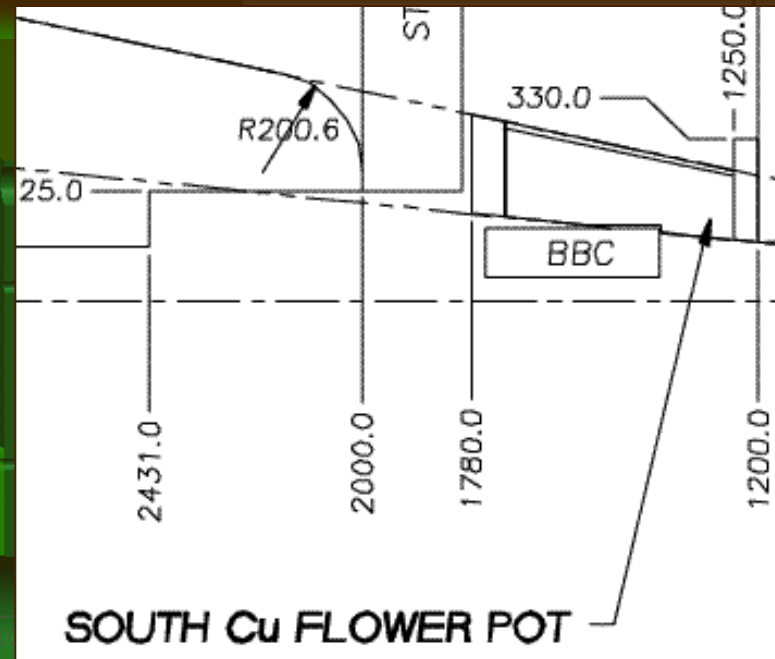


- Tracking detectors measures charged particle trajectory and momentum
- Calorimeter layers measure energy by fully absorbing the particles (destructive measurement).
- Muons do not interact in calorimeter very much: outermost detector to identify muons.



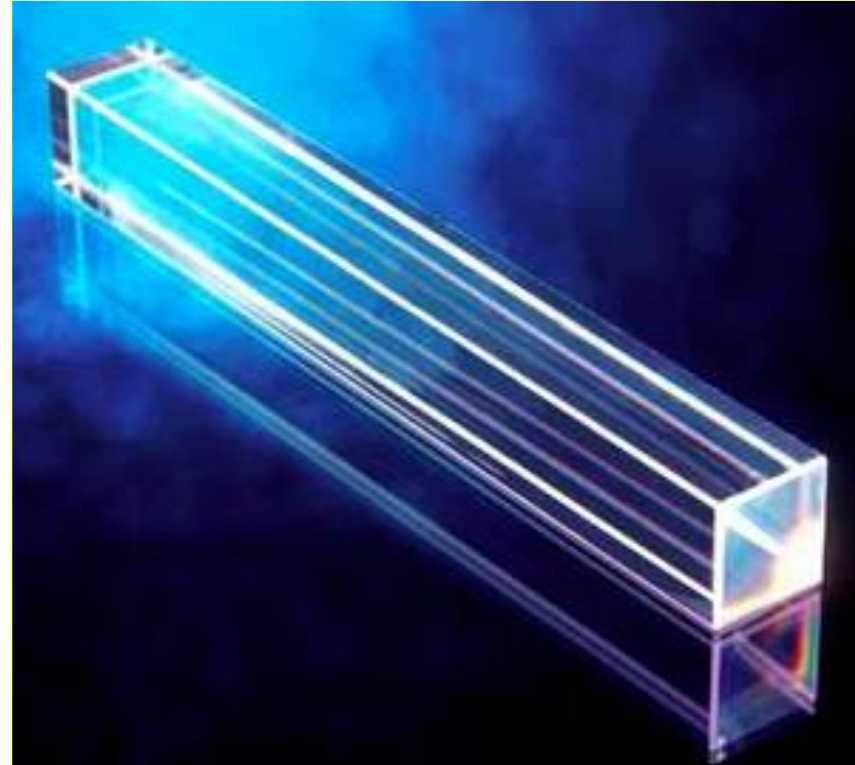
Space in muon piston holes!

Piston hole
41.3 cm long
22.5 cm radius



PbWO₄ (Lead Tungstate, PWO)

Density	8.28 g/cm ³
Size	2.2 x 2.2 x 18 cm ³
Length	20 X ₀ , 0.92 λ
Weight	721.3 g
Moliere radius	2.0 cm
Radiation Length	0.89 cm
Interaction Length	22.4 cm
Light Yield	~10 p.e./MeV @ 25° C
Temp. Coefficient	-2% / °C
Radiation Hardness	1000 Gy
Main Emission Lines	420-440, 500 nm
Refractive Index	2.16



about 50 years in PHENIX
forward directions

Avalanche photodiodes?

Even small PMTs are sensitive to magnetic fields or expensive
(500 – 5000 gauss longitudinally in piston holes)

PIN diodes

in reverse bias mode → depleted i-layer

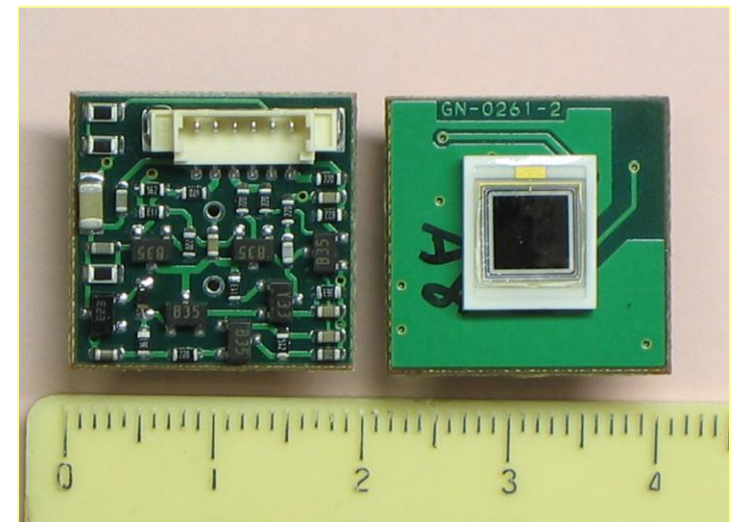
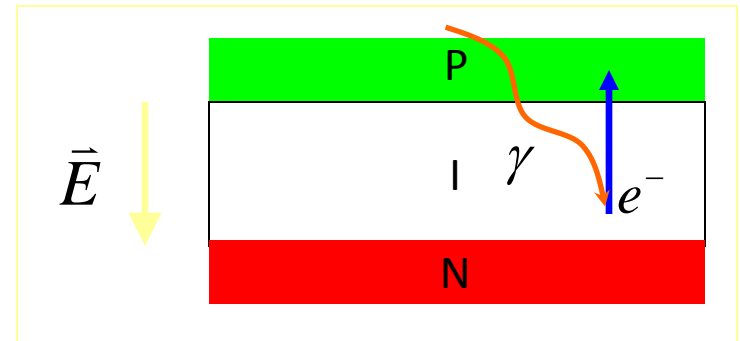
Large reverse bias voltage:

e^- acceleration

→ collisions with electrons

avalanche multiplication

avalanche leaves the active area



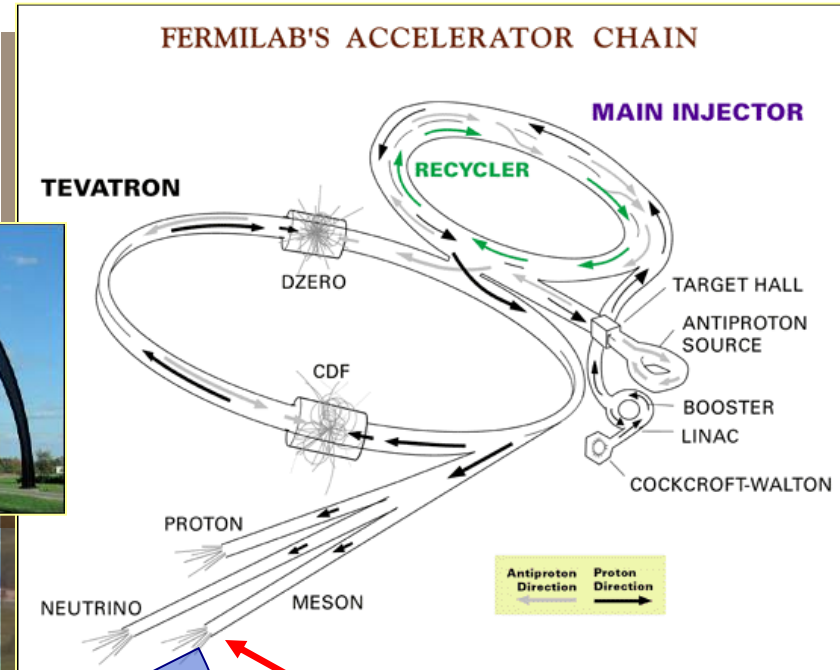
Test beam measurements

MTBF @ FNAL

Test beam from 4 GeV/c to 120 GeV/c

Pion or electron tune

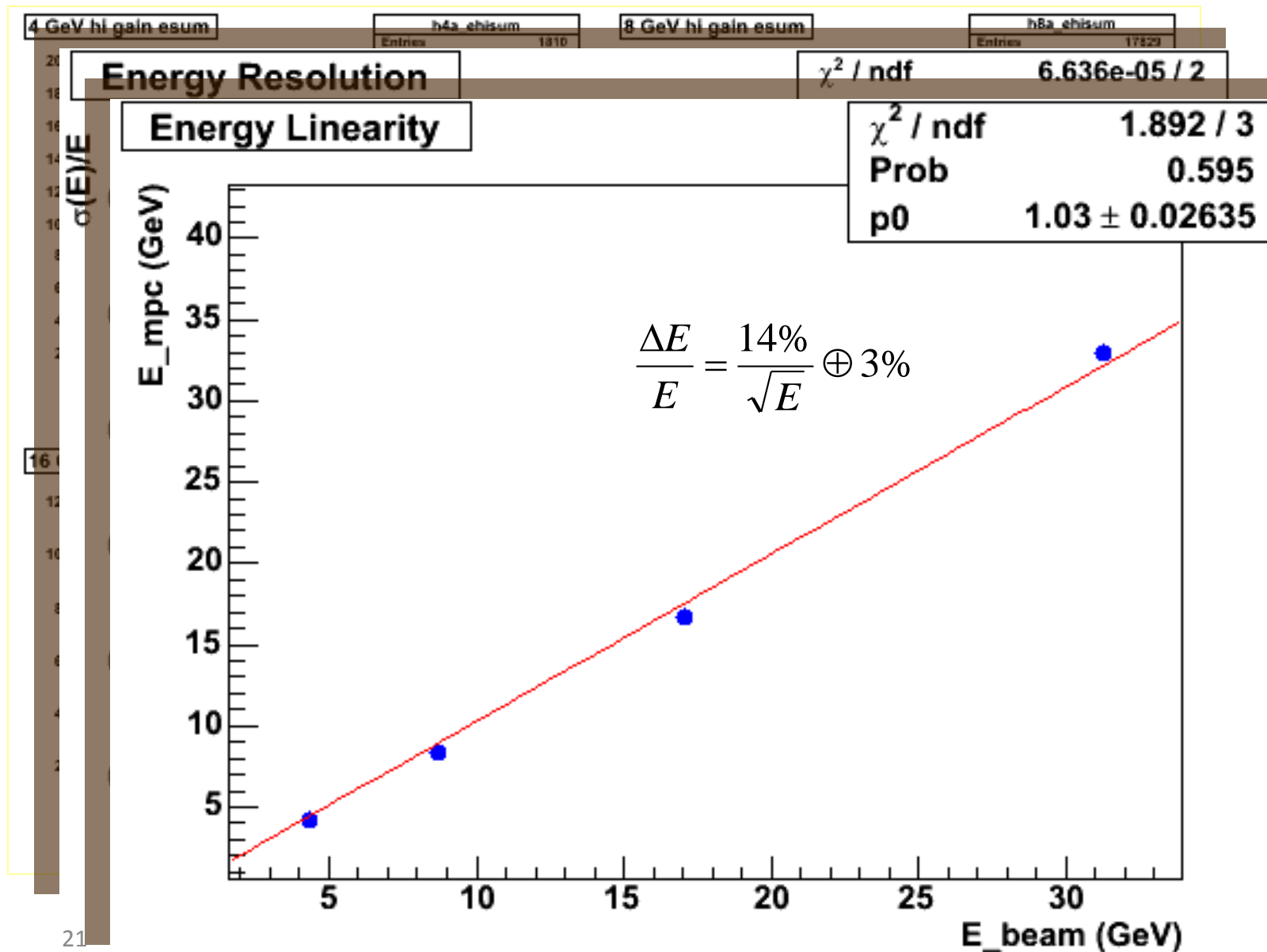
Electron / hadron ID in RICH



Al target



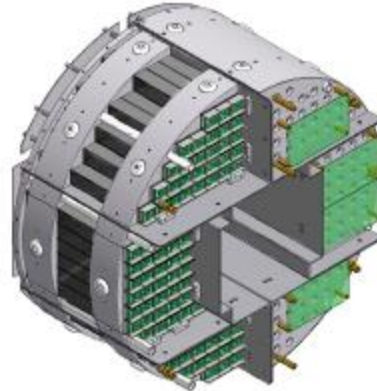
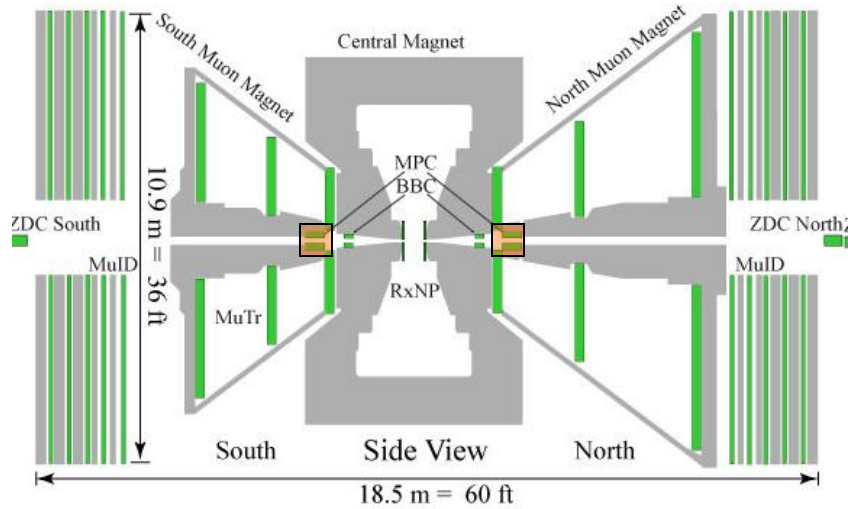
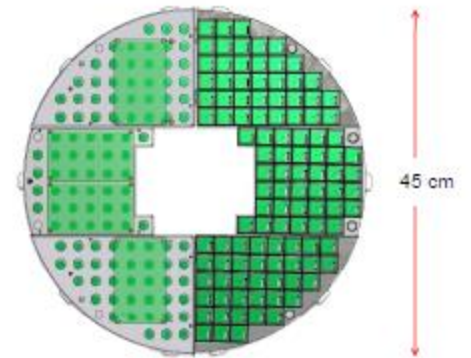
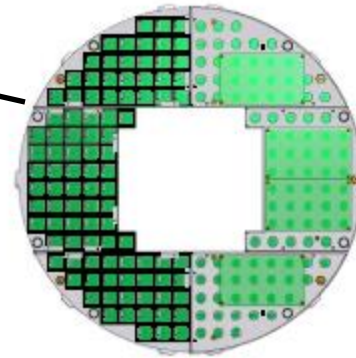
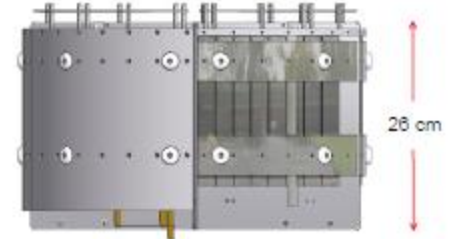
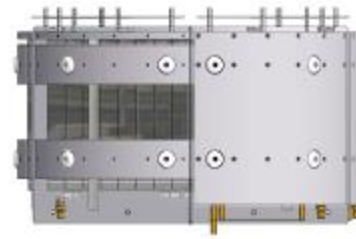
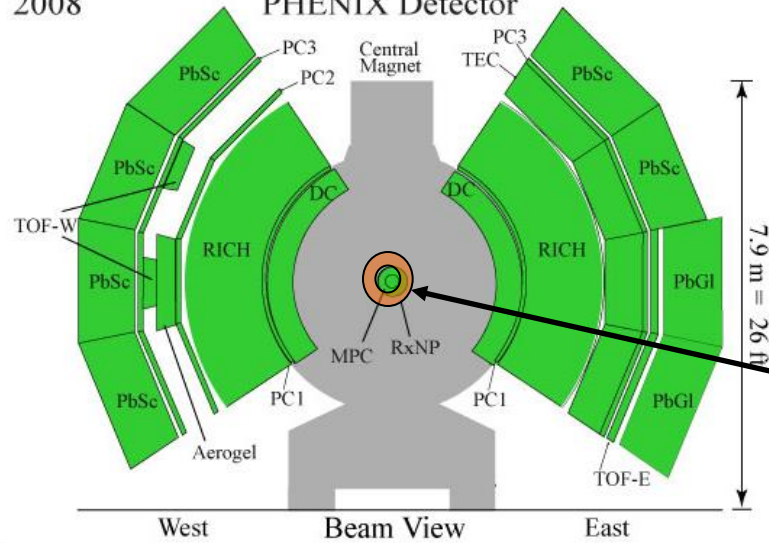
FermiLab Test Beam Results



The MPC: $3.1 < |\eta| < 3.8$

2008

PHENIX Detector

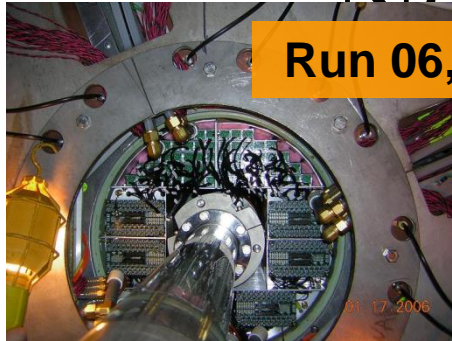


MPC History

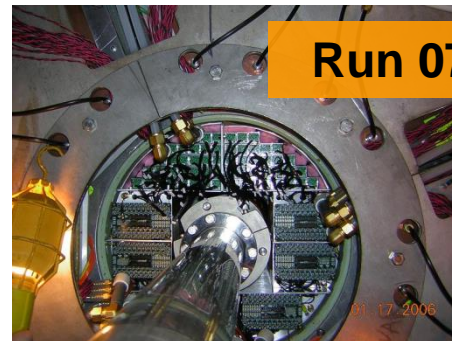
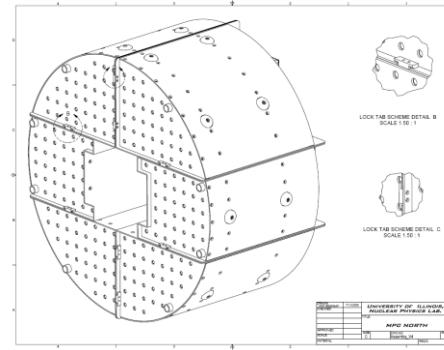
South

North

Initial Installation
192 Towers



Run 06, pp: 200, 62 GeV



Run 07, AA: 200 GeV



New Detector:
220 Towers

Upgrade:
196 Towers
New Monitoring
System (N+S)



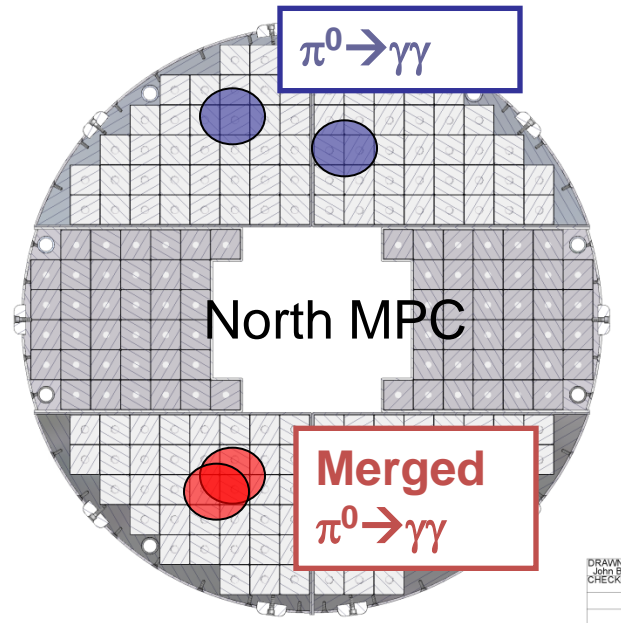
Run 08, dA, pp: 200 GeV



Light Calibration Box



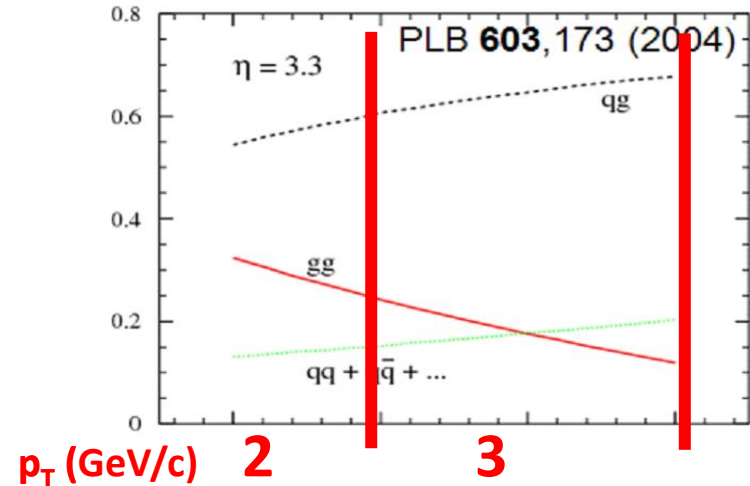
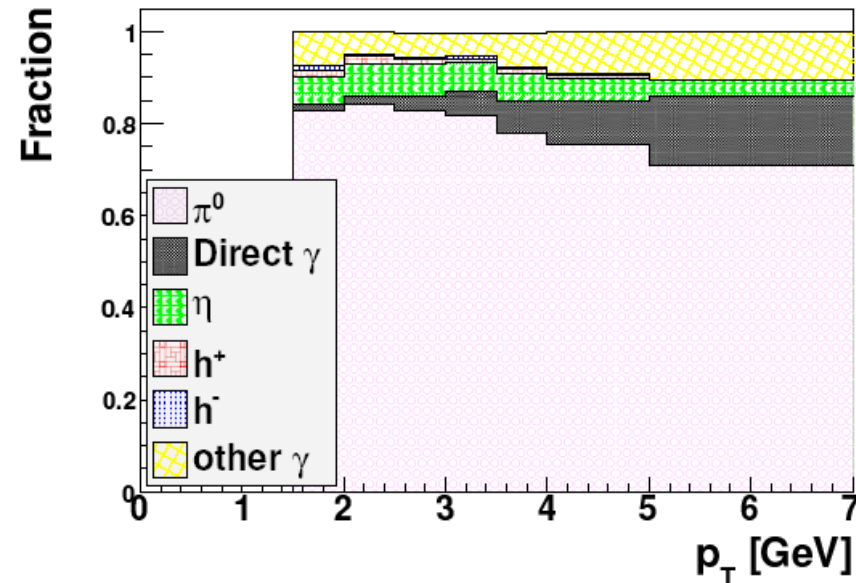
MPC Limitation



- ID π^0 s up to $E \sim 20$ GeV with MPCs ($3.1 < |\eta| < 3.8$)
 - Limitations: tower separation and merging effects
 - **Use π^0 s for $7 \text{ GeV} < E < 22 \text{ GeV}$**
 $\rightarrow p_T \text{ max} \sim 2 \text{ GeV}/c$
- **Single Clusters for $E > 15 \text{ GeV}$**
 - **Dominated by π^0 ($\sim 85\%$)**
 - **Access higher p_T**

Single Cluster Asymmetry

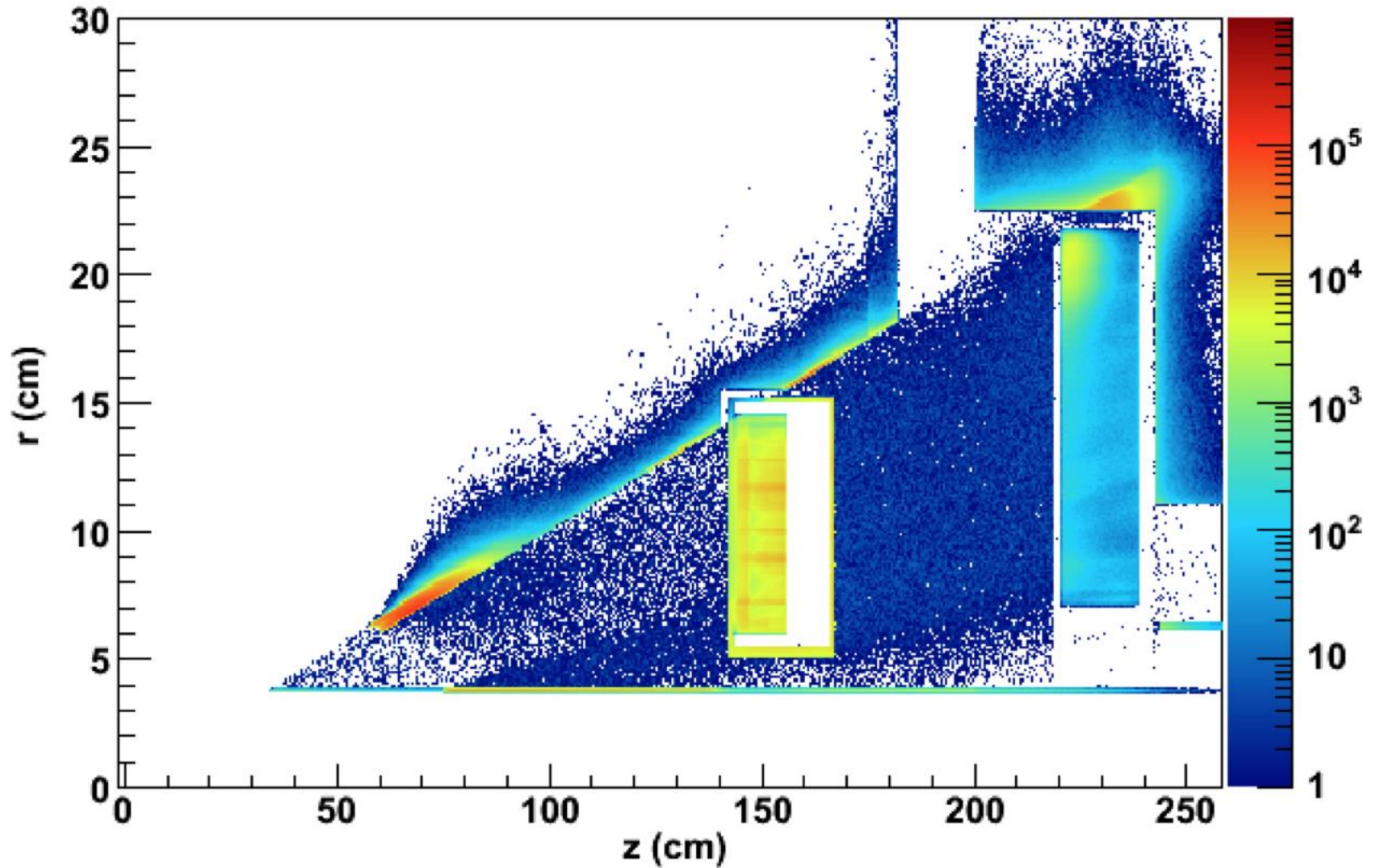
Cluster Decomposition: Dominated by merged π^0 's.



- ✓ Process decomposition skewed more heavily toward quark-gluon than mid-rapidity.
- ✓ Rel lumi uncertainty is significant compared to statistical.

Hits r vs z

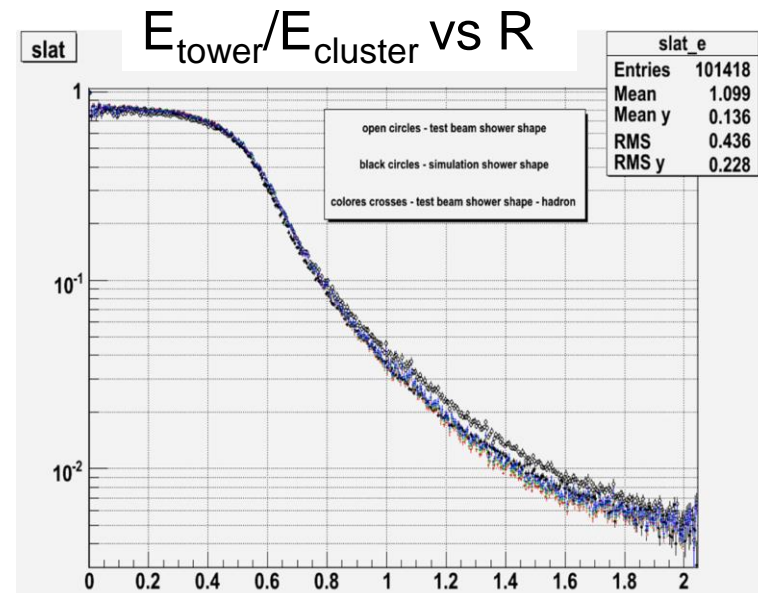
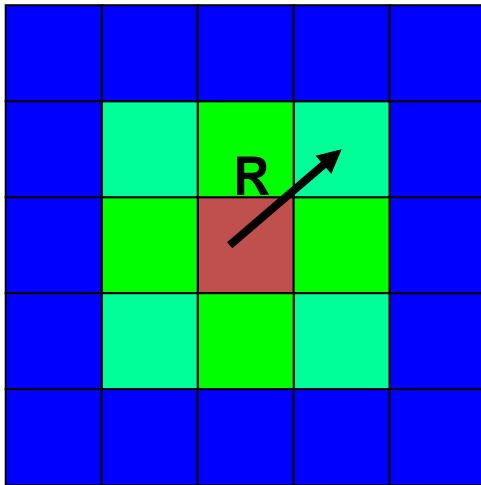
“Albedo”



MPC is in a very messy environment! Over a radiation length in front of it.

Reconstruction Algorithm (AN949)

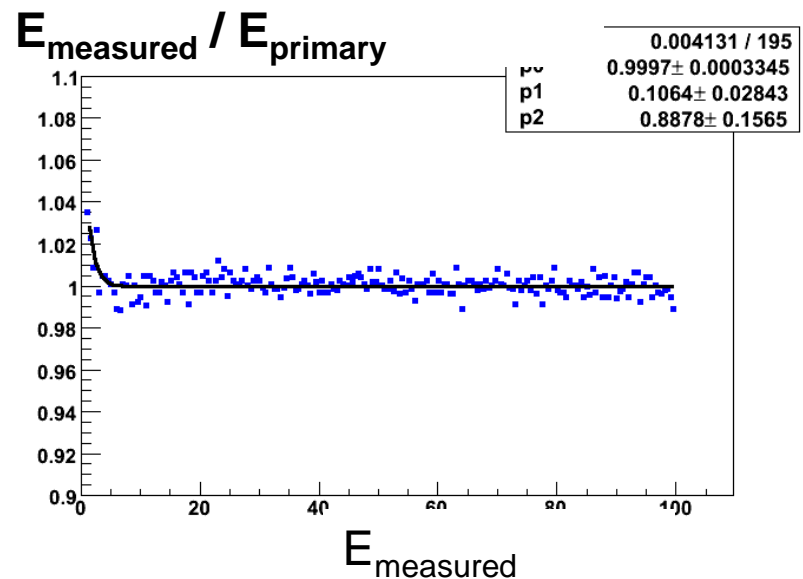
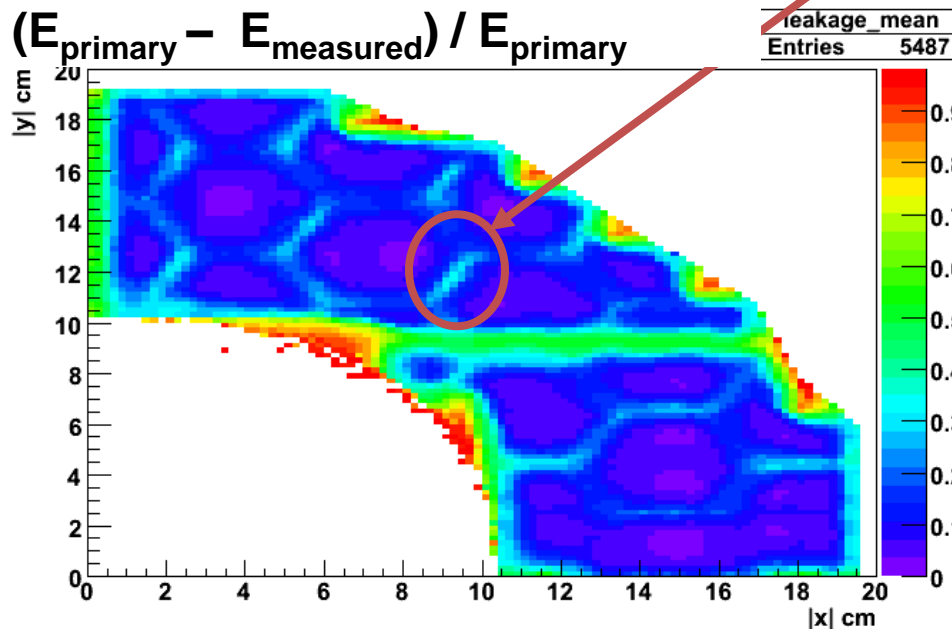
- Basic idea: EMCal clusters = local maxima + surrounding towers
- Use log-weighted positions (weight is $4 + \ln(E_i/E_{\text{tot}})$)
- Adapted existing EMCal code to MPC
- Parameterize shower shape and fluctuations from simulation (matches beam test well)



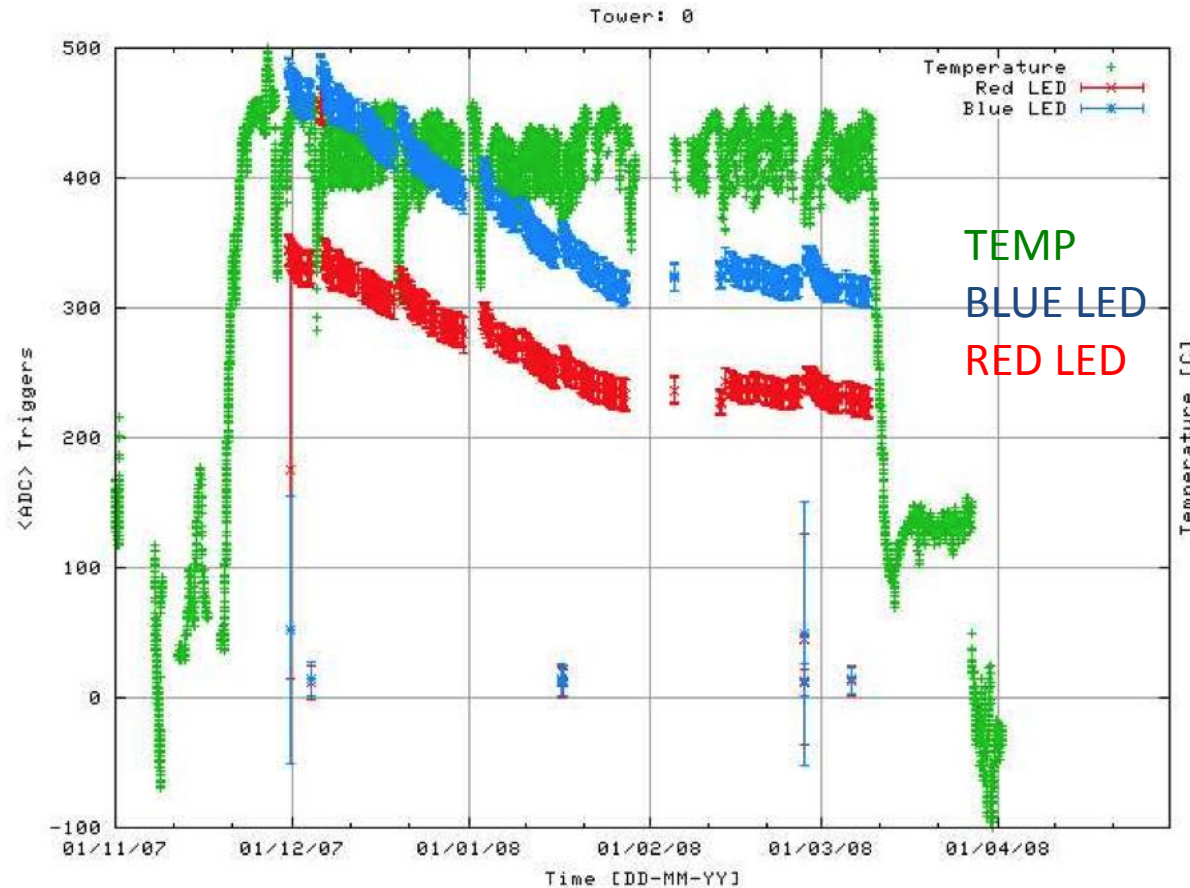
R = distance from tower center to cluster center

MPC Energy Response

- MPCs sit directly behind the BBCs (see shadow below from $E = 20$ GeV single photons run through GEANT)



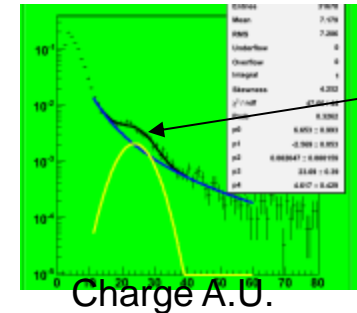
MPC Gain Drop During Run



- PbWO4 and APD gains both sensitive to temperature
- PbWO4 suffers massive radiation damage
 - Recovers partially between runs
- APD also suffers neutron damage – not recoverable
- LED essential to correcting for this gain drop and fluctuations in gain

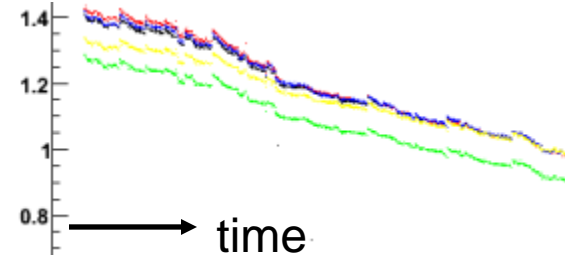
Calibrations (our 3rd iteration) AN927

- Use Minimum ionizing particles as first calibration (MIPs deposit 0.234 GeV/tower)
 - Also can use inverse slopes
- Correct time-dependence with LEDs (40% over 2008 d+Au, p+p runs)
- Use iterative π^0 calibration
 - Match p+p pythia \rightarrow GEANT simulation masses in each tower



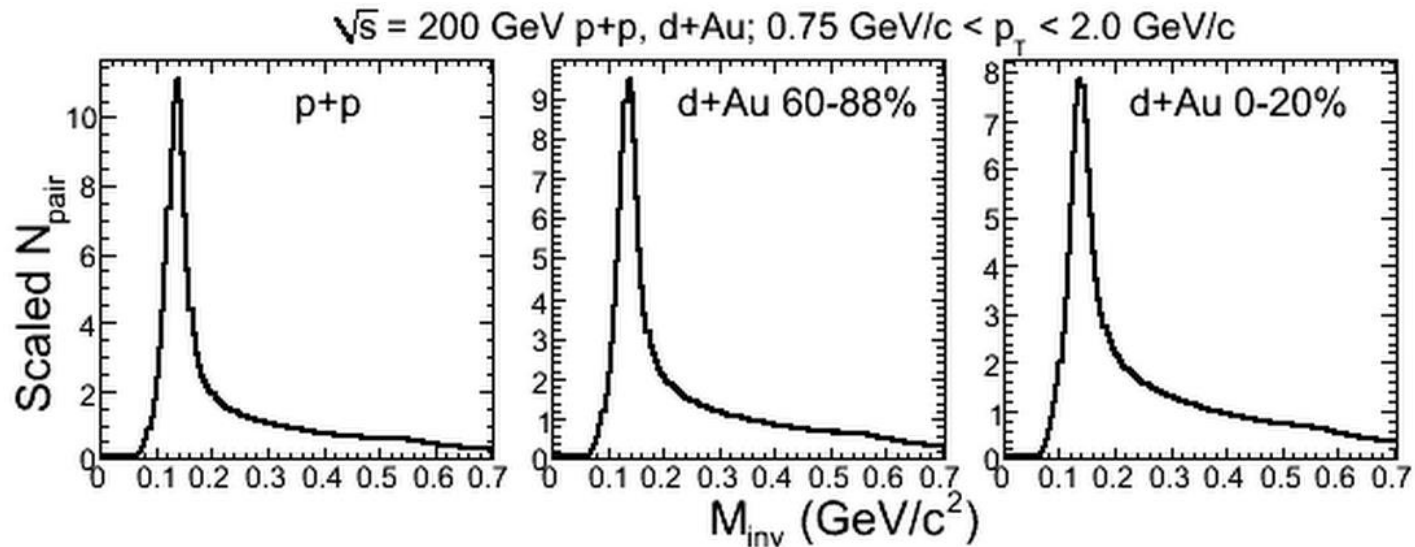
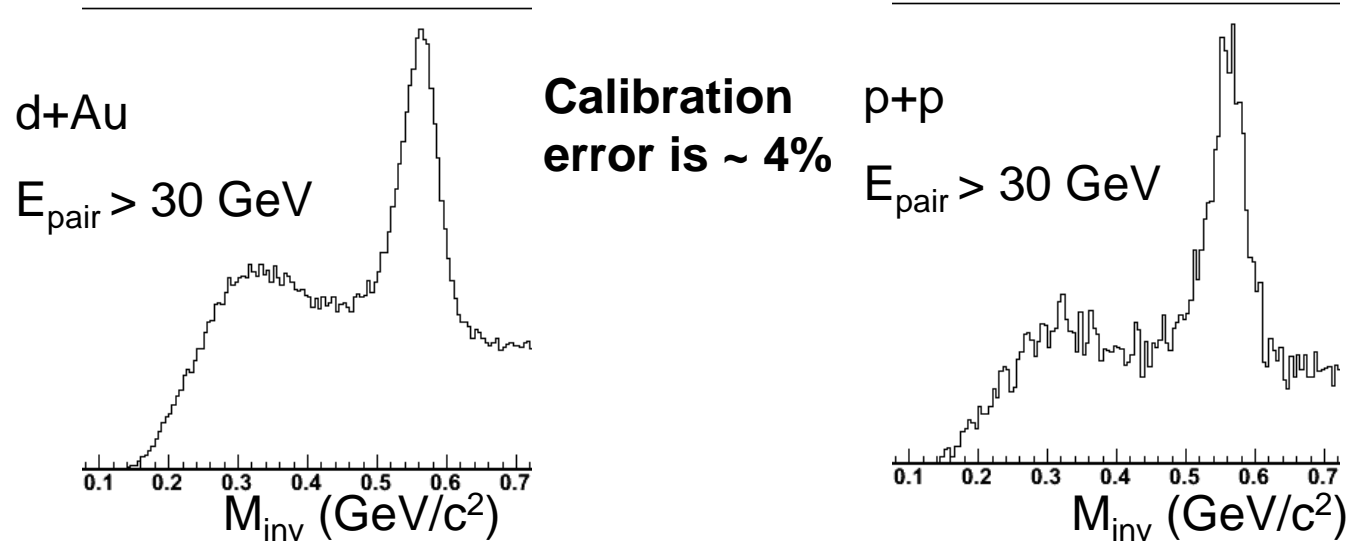
MIP
peak

2008 Led variation vs time



Tower by tower π^0
mass peaks

Tests of Calibration: η and π^0 mesons



Tests of Simulation

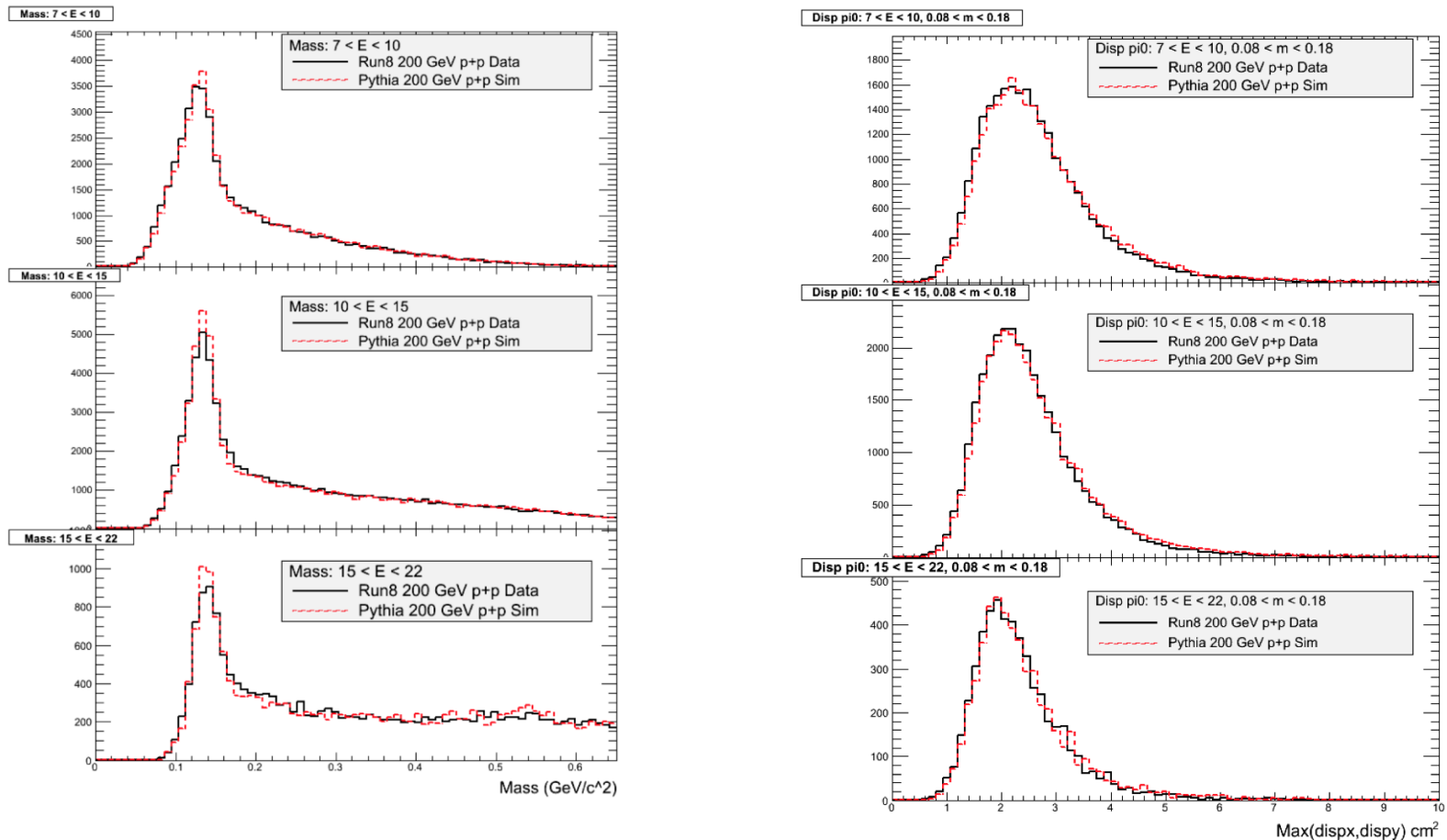


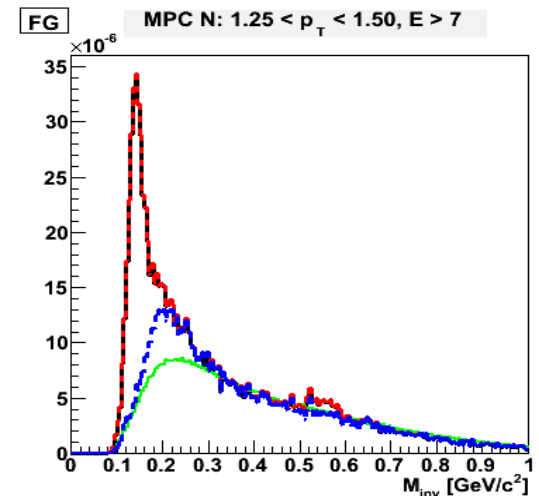
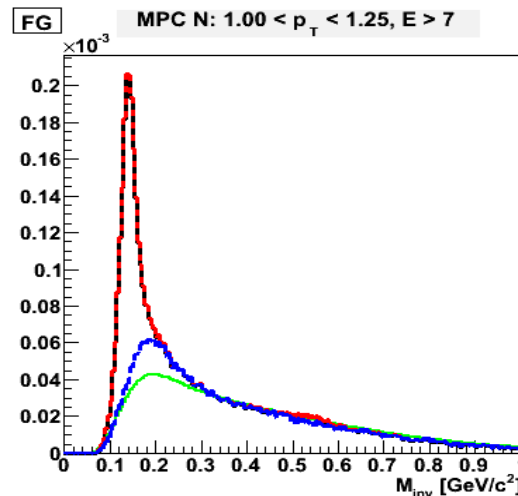
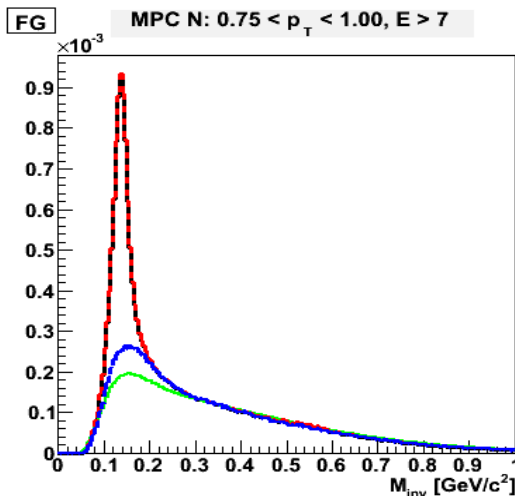
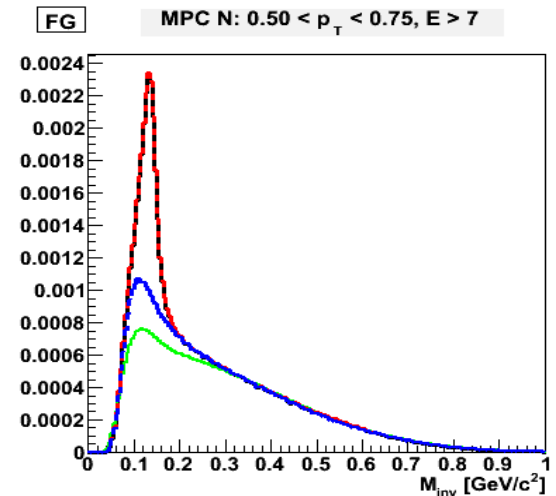
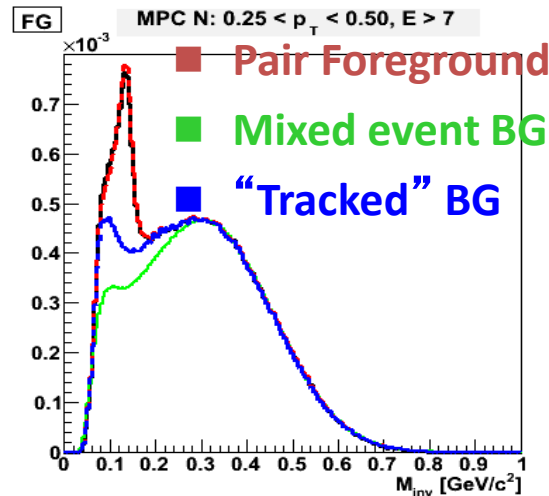
Figure 7: North MPC invariant mass vs. energy

- Simulation should match the data if one wants to use the simulation for correction factors
- North MPC, Run08 p+p

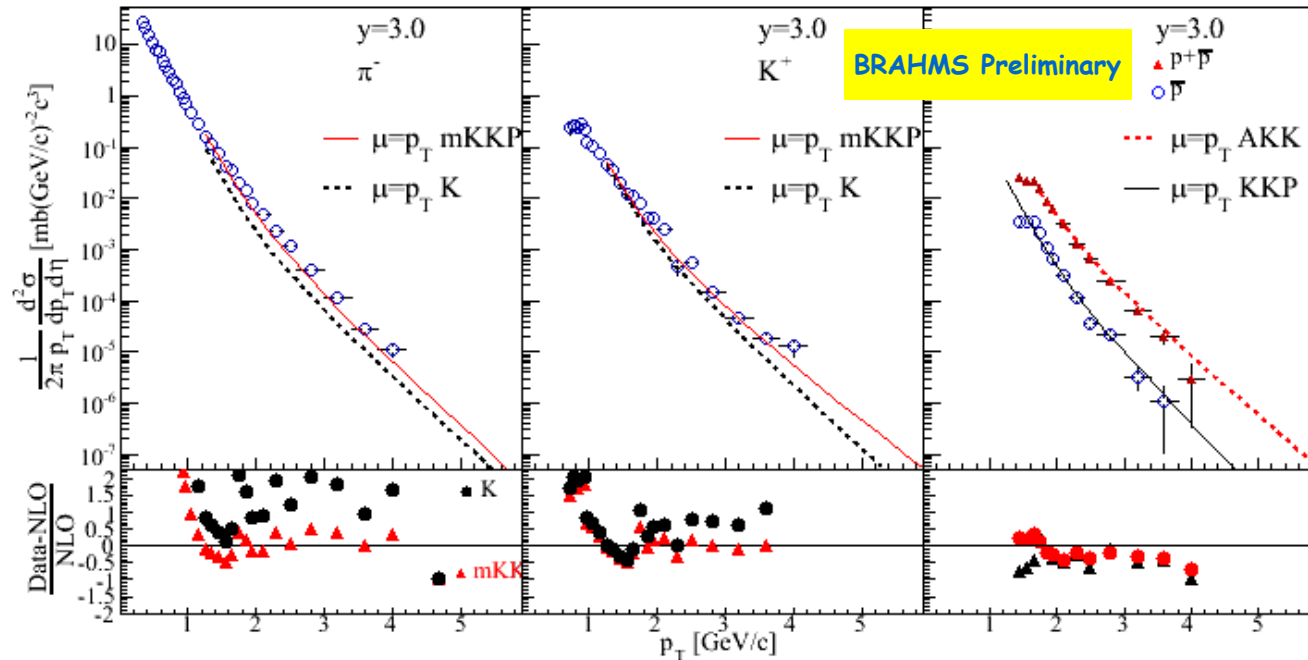
Understanding the Invariant Mass Spectra

- Developed tools to understand invariant mass spectra
- Track energy depositions for all particles into clusters
- Tracking available in mpcClusterContentV2

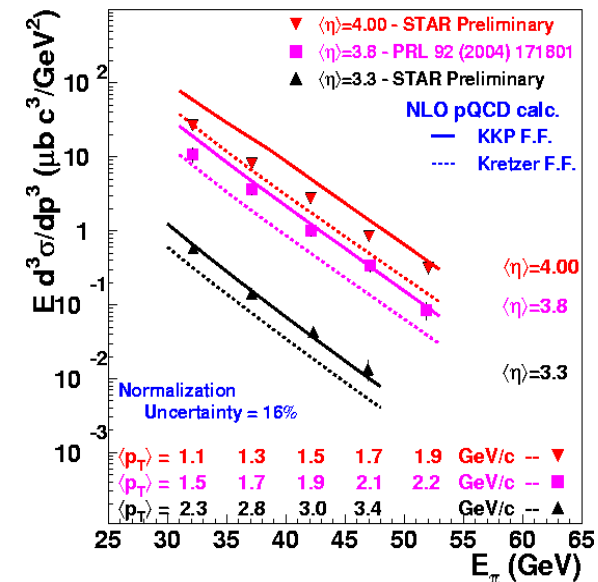
2 embedded p+p Pythia events \rightarrow PISA \rightarrow DST



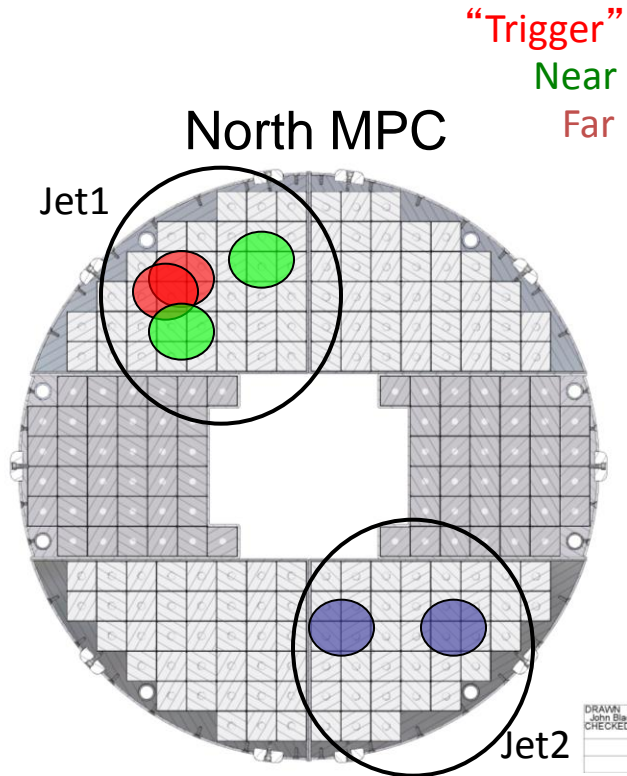
Cross-sections at RHIC, Forward Rapidities



- Cross-sections generally described well by NLO pQCD at $\sqrt{s} = 200$ GeV and forward rapidities
- Are we in a situation where in unpolarized the theory is relatively well understood, but the polarized gives surprises?
 - Potentially we are in a region where the polarized data gives us new information about QCD, in a region where one can have quantitative theoretical understanding of the effects, and not just phenomenology.

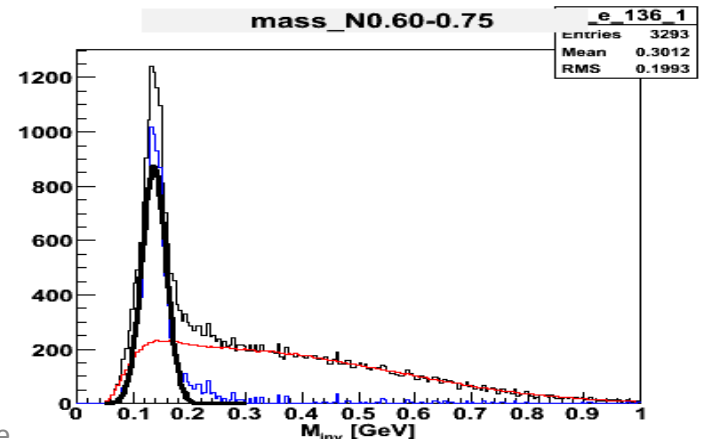
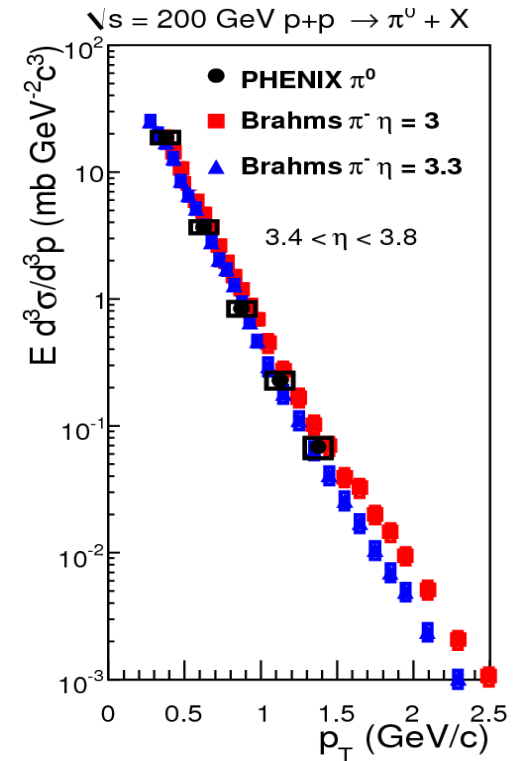
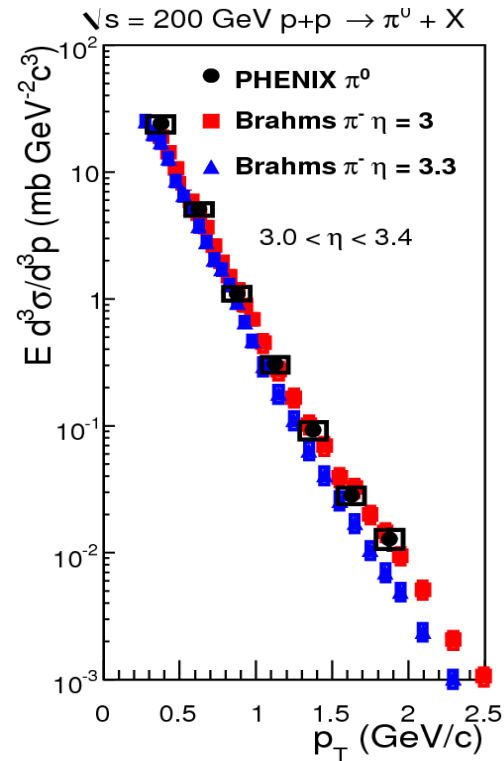


MPC Performance

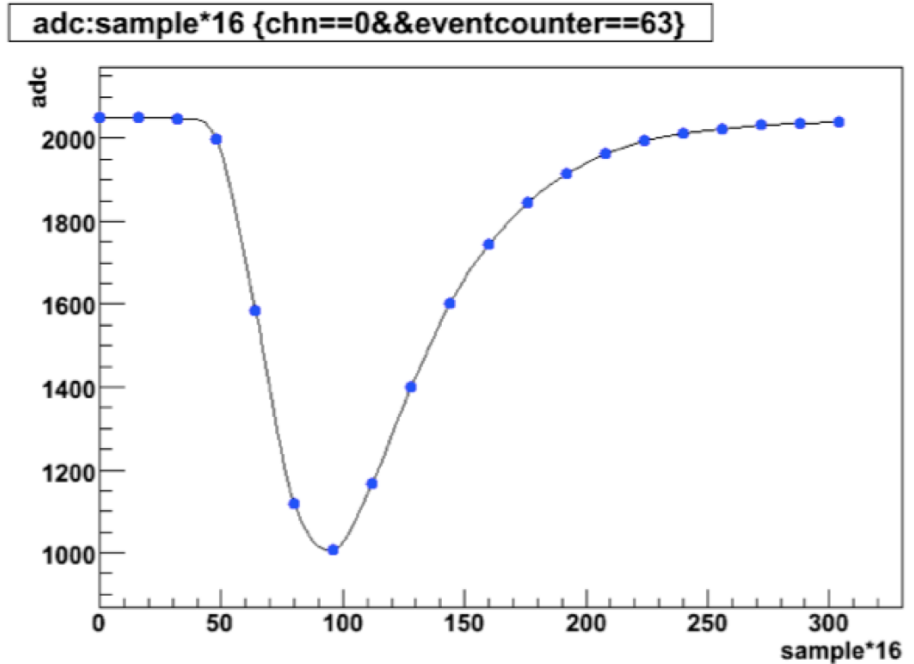
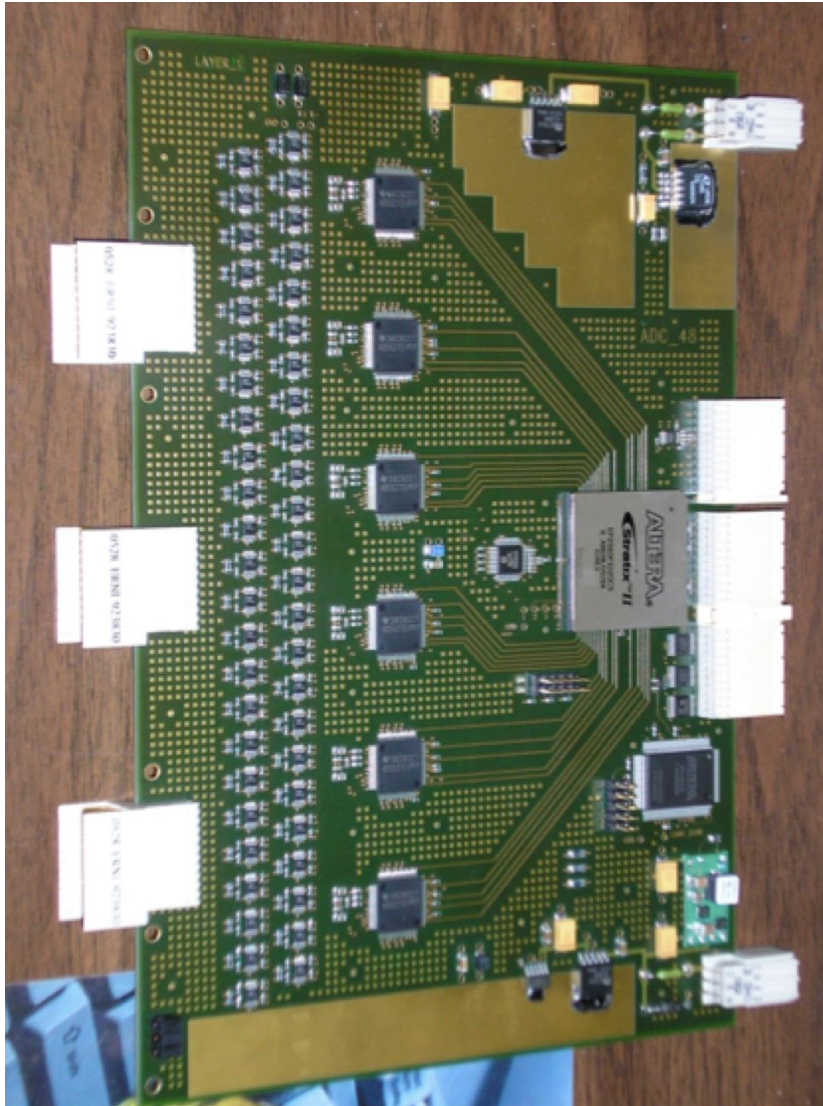


Decay photon impact positions for **low** and **high** energy π^0 s. The decay photons from **high** energy π^0 s merge into a single cluster

Clusters $\geq 80\% \pi^0$ (PYTHIA)



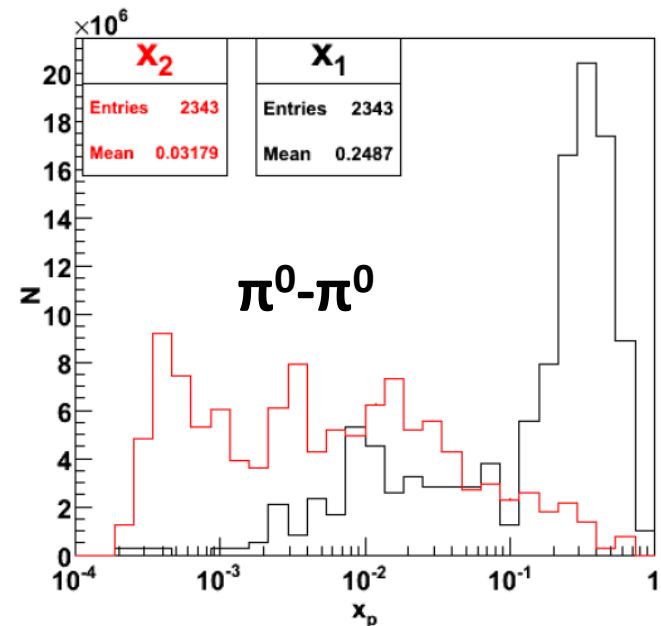
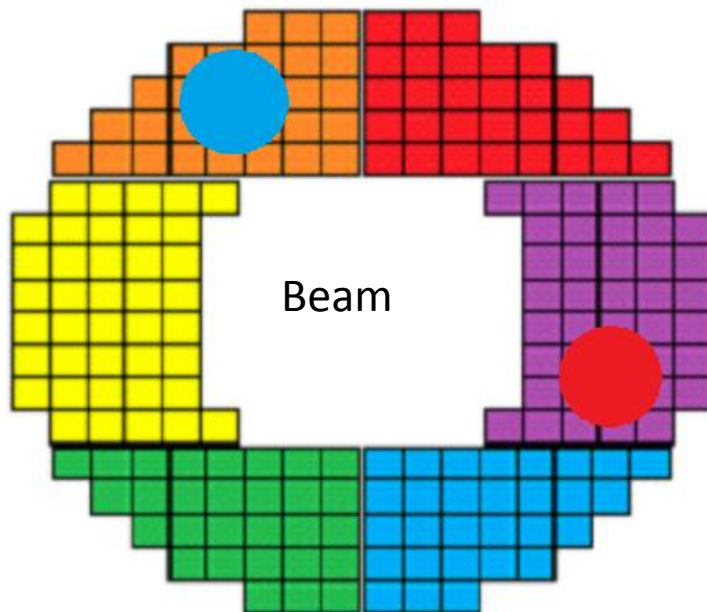
Upgraded Electronics in Run12



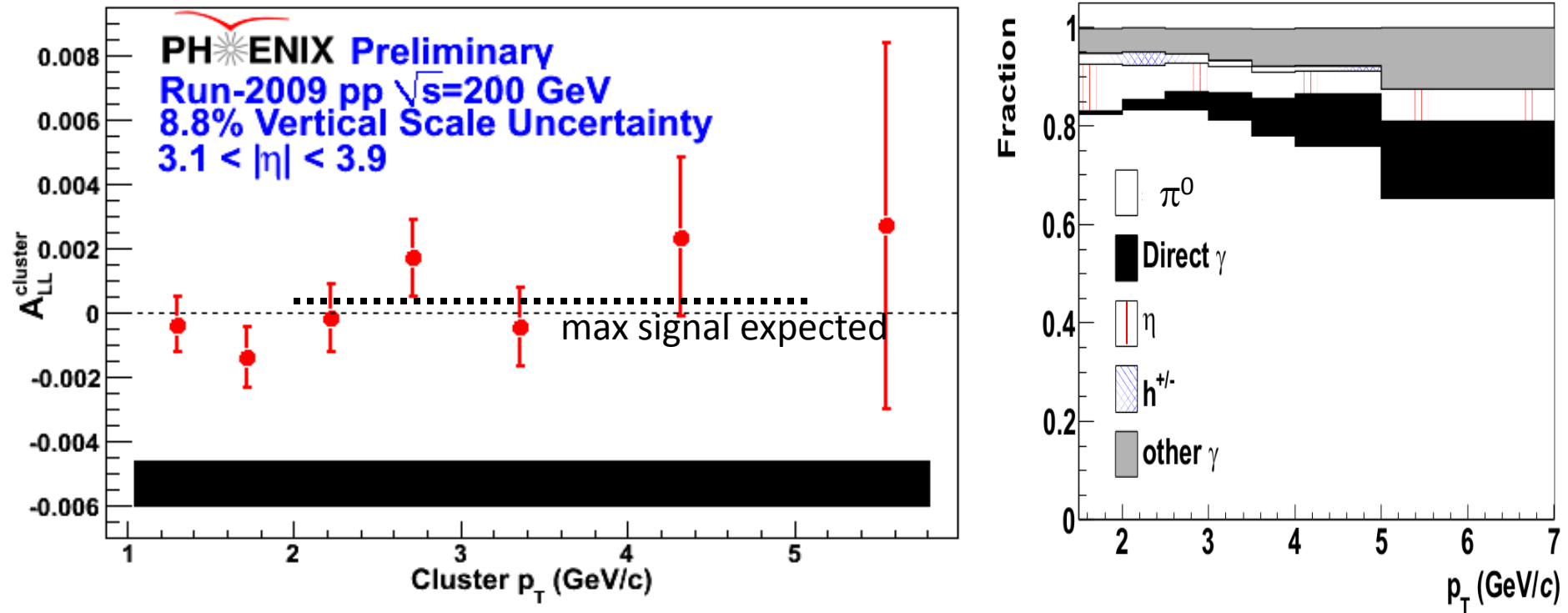
- New electronics in Run12 (HBD ADC boards)
- Digital trigger
 - pT threshold
 - Online gain corrections
 - Remove single tower backgrounds
- Measure energy beyond ADC saturation
- Controls pileup effects

Trigger on Di-hadrons

- MPC now has 6 independent fully digital trigger calculations, arranged azimuthally
- Easy to select for di-hadrons → Increased rejection power
- Allows us to maximize our data purity
- Constrain ΔG at low- x , and with less inclusive probe.

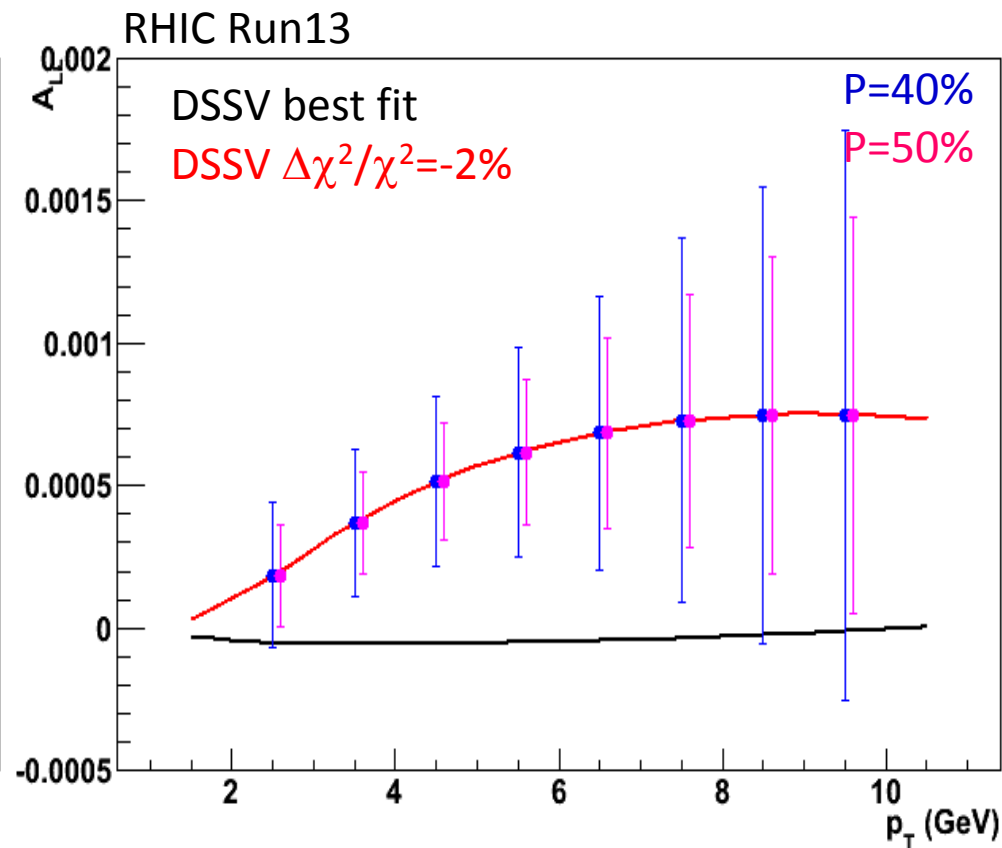
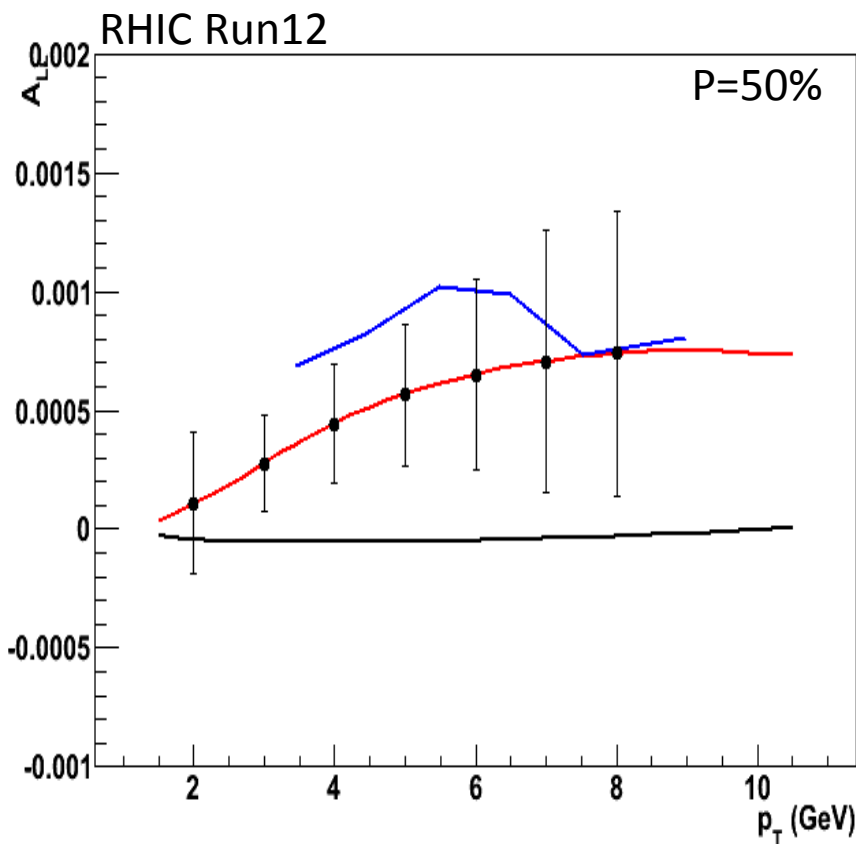


First Forward Measurement of A_{LL}



- High p_T EM Cluster Asymmetry, forward pseudo-rapidity $3.1 < |\eta| < 3.9$
 - >80% Merged π^0
- 510 GeV Datasets: Run09, Run11, Run12, Run13
 - Run12 and Run13 use new MPC electronics with $\sim 4\times$ higher purity

Run12, Run13 Projections



- Projected error bars around $\delta A_{LL} \sim 10^{-4}$
- From real data, with new MPC Trigger Electronics
- Relative Luminosity Analysis still in progress

Can Clusters be Used?

1. Assign a systematic error
 - We have a good idea about the particle type composition
 - Be nice to measure eta's and direct photons separately. Pi-zero's already measured by STAR.
 - We can then calculate what kind of an effect these have on the A_{LL} given certain assumptions about dG
 - Derive a conservative systematic error based on that
2. Try to correct back to pi-zero's
 - Similar to above, but we also apply a correction based on some assumed dG, and assign systematic errors to the uncertainty in that correction.
3. Give the theorists our acceptance and efficiency for each particle type
 - With this information they can run this $acc*eff$ filter through their analysis.